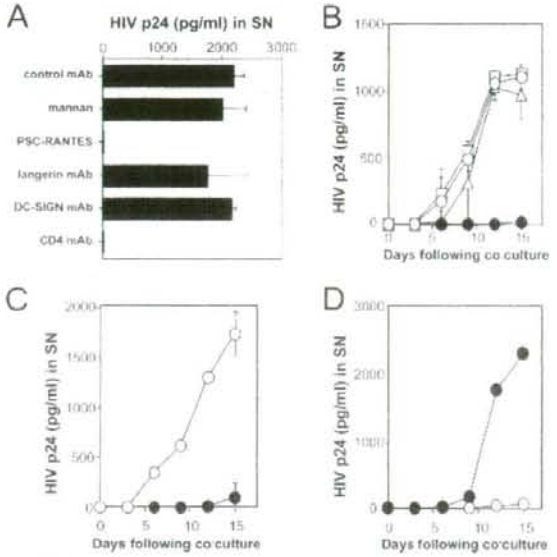

FIGURE 2. After epidermal exposure to HIV, HIV-infected LC from virus-exposed skin transmit infection to T cells. *A* and *B*, The surfaces of abraded skin were preincubated with PSC-RANTES (200 nM) (●), mannose (200 μg/ml) (□), mannan (200 μg/ml) (Δ), no reagents (○), or indicated Abs (40 μg/ml) before epidermal exposure to HIV-1_{Ba-L}. Emigrant cells from each experiment were cocultured with allogeneic $CD4^+$ T cells. *C*, The epidermis and dermis of HIV-exposed skin were separated. Cells emigrating from epidermal (○) or dermal (●) sheets were cocultured with allogeneic T cells. *D*, Emigrating cells from HIV-exposed skin explants were collected, and half the emigrants were depleted of LC by immunomagnetic bead separation. Nondepleted (●) and LC-depleted (○) emigrants were cocultured with allogeneic T cells. HIV p24 levels in coculture supernatants (SN) were assessed by ELISA. Data shown represent at least two separate experiments derived from separate donors.

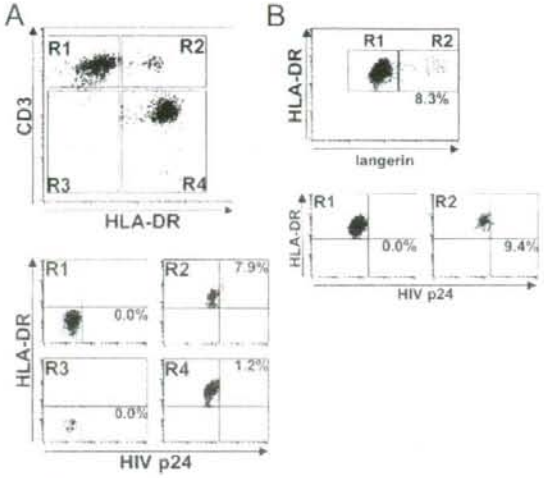

FIGURE 3. HIV infection within LC, but not within dermal DC. Emigrating cells from HIV_{Ba-L}-exposed skin explants were stained for the surface Ags shown or intracellular HIV p24. HIV p24 staining of each gated population in emigrating cells (*A*) or HLA-DR^+ emigrant cells (*B*) is shown. Emigrating cells from control skin explants unexposed to HIV were always negative for p24 staining (data not shown). Data shown are representative of three separate experiments derived from three separate donors.

LC play a critical role in virus dissemination from skin emigrants to T cells.

HIV-infected cells were detected in LC, but not in dermal DC or macrophages, emigrating from R5 HIV-exposed skin explants

Others have shown that emigrating cells from skin explants contain three main populations of cells, as follows: HLA-DR^+CD3^- LC/DC, $CD3^+$HLA-DR^- T cells, and HLA-DR^+CD3^+ LC/DC-T cell conjugates (31, 33). To determine which populations are infected by R5 HIV using our new model, HIV_{Ba-L} was applied to the surface of abraded skin explants and the emigrating cells from the explants were stained with intracellular HIV p24. The number of LC/DC and T cells emigrating from the explants was variable, depending on the donor. In a series of five experiments, analysis of the emigrant cells showed a mean ± SD of 22.9 ± 8.3% T cells, 17.7 ± 9.5% LC/DC-T cell conjugates, and 35.1 ± 14.5% LC/DC. HIV $p24^+$ cells were detected in HLA-DR^+ populations: LC/DC and LC/DC-T cell conjugates, but not in HLA-DR-negative populations (Fig. 3*A*). To determine which DC/macrophage subsets (i.e., $CD1a^+$langerin$^+$DC-$SIGN^-$ LC, $CD1a^+$langerin$^-$DC-$SIGN^-$ dermal DC, and $CD1a^-$ langerin$^-$DC-$SIGN^+$ dermal macrophages observed in Fig. 1*A*) are infected by HIV, HLA-DR^+ cells migrating from HIV-exposed skin were further analyzed for infection. Interestingly, we could detect HIV $p24^+$ cells in langerin$^+$ LC (R2), whereas langerin$^-$ DC/macrophages (R1) demonstrated <1% HIV-infected cells (Fig. 3*B*). In three experiments in which HIV-infected emigrant cells were characterized, the results for percentage of HIV $p24^+$ cells in LC vs dermal DC/macrophages were 9.4 vs 0.0%, 5.6 vs 0.8%, and 12.2 vs 0.1%, respectively. These results suggest that LC are the major target for HIV infection when the epidermal surface of abraded skin is exposed to virus. Variability in LC infection levels may be due to CCR5 heterogeneity in skin donors, as documented by previous findings (23). In this model, disruption of the corneal layer of the epidermis was necessary for infection, because no HIV-infected cells were detected in the migrating cells when virus was applied to the surface of nonabraded skin (data not shown).

HIV replicates within LC emigrating from R5 HIV-exposed skin explants

Recently, we established an ex vivo model whereby resident LC within epithelial tissue explants are exposed to R5 HIV and found productive virus infection of LC, as evidenced by the following observations: 1) positive staining for HIV p24, 2) virions budding from cell surfaces, and 3) detection of HIV transcripts (22–24, 34–36). To test directly whether HIV can replicate within LC, skin explants were exposed to HIV variants that were engineered to express GFP during productive infection of cells. $NLCSF_{V3}EGFP$ (an R5 virus) was applied to the surface of abraded skin explants. Six days following virus exposure, we could detect GFP-positive large cells with dendritic morphology in emigrant cells (Fig. 4*A*). When the emigrants were stained with anti-langerin and anti-CD3 mAb, GFP^+ cells could be seen in langerin$^+$ $CD3^-$ LC and langerin$^+$ $CD3^+$ LC-T cell conjugates (R1 and R2) (Fig. 4*B*). Although T cells within the emigrants were never GFP^+, more brightly GFP^+ LC were occasionally observed in clusters of cells (Fig. 4*A*). When $NLCSF_{V3}EGFP$ was added to the entire skin explants, GFP^+ cells were detected in LC and in langerin-negative dermal DC or macrophages (data not shown). To test whether LC replicate HIV without interaction with T cells, LC within epidermal sheets were exposed to $NLCSF_{V3}EGFP$. Three days following

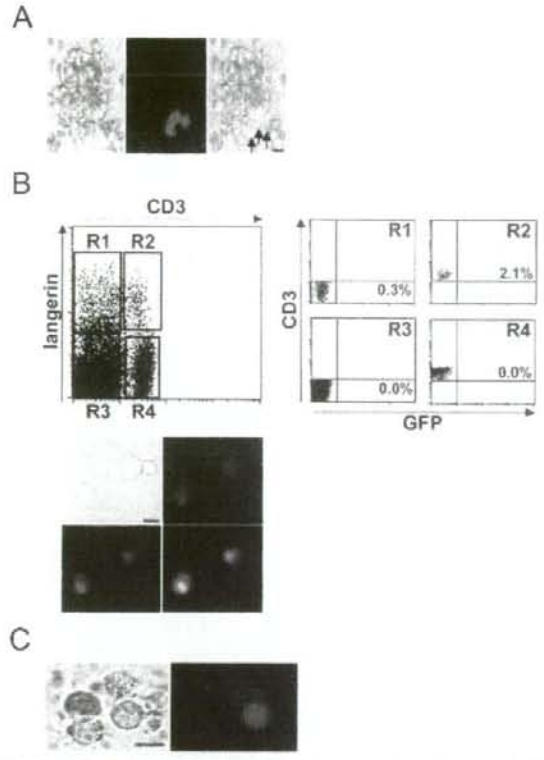

FIGURE 4. R5 HIV replicates within LC. Skin explants (*A* and *B*) and epidermal sheets (*C*) were exposed to $NLCSF_{V3}EGFP$ (R5 HIV), and emigrating cells were examined under microscope or by flow cytometry. *A*, Microscopic (*left*) and fluorescence microscopic (*middle*) images of skin emigrants were combined (*right*). Representative $EGFP^+$ large DC (arrows) demonstrate expression of EGFP. *B*, Emigrating cells from skin explants were processed for flow cytometry following langerin and CD3 staining. GFP^+ cells of each gated population in emigrating cells are shown. Images derived with FITC (green: GFP) and rhodamine filters (red: langerin) were combined (yellow). *C*, Microscopic (*left*) and fluorescence microscopic (*right*) images of emigrating cells from epidermal sheets were shown. Emigrating cells from control skin explants or epidermal sheets unexposed to HIV were always negative for GFP (data not shown). Scale bar, 10 μm. Data shown represent at least two separate experiments derived from separate donors.

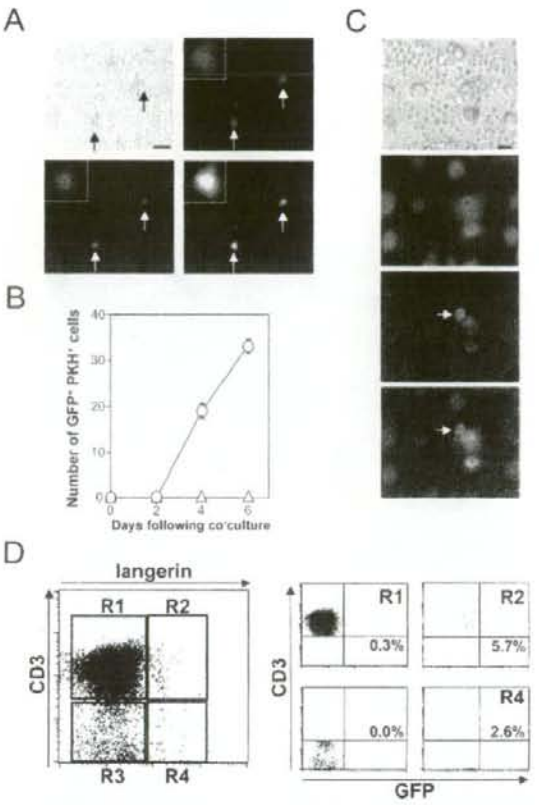

FIGURE 5. HIV transmission from LC to T cells. Emigrating cells from $NLCSF_{V3}EGFP$-exposed skin were labeled with PKH67 Red before being cocultured with T cells. Images derived with FITC (green) and rhodamine filters (red) were combined (yellow). Representative HIV-infected GFP^+PKH^+ LC (arrows, *A*) and HIV-infected GFP^+PKH^- T cells (arrows, *C*) are shown. *Insets* (*A*): higher magnifications. *B*, GFP^+ cells in PKH^+ cells were counted in the cocultures of emigrating cells from $NLCSF_{V3}EGFP$ (○)- or NL43EGFP (Δ)-exposed skin. In PKH^- cells, GFP^+ cells were not detected during the first week. Scale bar: *A*, 50 μm; *C*, 10 μm. *D*, The cocultures were processed for flow cytometry following langerin and CD3 staining. GFP^+ cells of each gated population in emigrating cells are shown. Data shown represent at least two separate experiments derived from separate donors.

virus exposure, GFP weakly positive cells with dendritic morphology were observed in emigrating cells from epidermal sheets (Fig. 4*C*). Because $CD3^+$ T cells were never detected in the emigrating cell populations (data not shown), this result indicates that low levels of productive R5 HIV infection occur in LC without interaction with T cells.

Visualization of viral transmission from HIV-infected LC to T cells

To visualize HIV transmission from LC to $CD4^+$ T cells, $NLCSF_{V3}EGFP$ (an R5 virus) or NL43EGFP (an X4 virus) was applied to the surface of abraded skin explants, and emigrating cells from HIV-exposed skin were labeled with PKH67 Red before coculture with allogeneic T cells. In the cocultures of emigrants from $NLCSF_{V3}EGFP$-exposed skin and T cells, we could detect GFP expression within PKH^+ large cells with dendritic morphology (i.e., HIV-replicating LC), and the number of GFP^+ LC progressively increased over the first week (Fig. 5, *A* and *B*). By contrast, we could not detect GFP^+ cells within the coculture of emigrants from NL43EGFP-exposed skin and T cells (Fig. 5*B*). Between day 10 and 12 following coculture of emigrants from $NLCSF_{V3}EGFP$-exposed skin and T cells, a number of GFP^+PKH^- small T cells was visible in cocultures (Fig. 5*C*). PKH^- T cells expressing high levels of GFP were found adjacent to PKH^+GFP^+ LC, suggesting that HIV-infected LC directly transmitted HIV to T cells (Fig. 5*C*). When the cocultures were stained with anti-langerin and anti-CD3 mAb, GFP^+ cells were detected in $langerin^+$ LC, $CD3^+$ T cells, and $langerin^+$ $CD3^+$ LC-T cell conjugates (R1, R2, and R4) (Fig. 5*D*).

R5 HIV, but not X4 HIV, applied to skin explants induces HIV infection in T cells cocultured with skin emigrants

To compare the efficiencies of R5 HIV and X4 HIV dissemination using our new model, viral inoculates containing 10,000 $TCID_{50}$

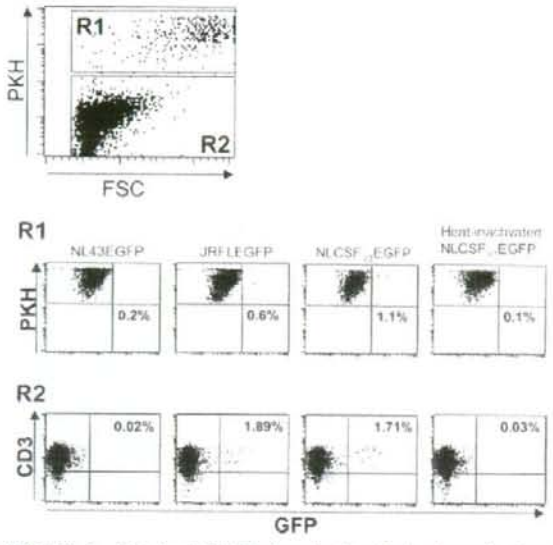

FIGURE 6. Selective R5 HIV dissemination. Emigrating cells from skin explants exposed to the indicated HIV strains were labeled with PKH67 Red before coculture with T cells. Cultured cells were stained with anti-CD3 mAb and analyzed by flow cytometry. PKH^+ (R1) or PKH^- (R2) cells were gated and further examined for GFP expression in each population. Data shown represent at least two separate experiments derived from separate donors.

of $NLCSF_{V3}EGFP$ (R5 HIV), JRFLEGFP (R5 HIV), or NL43EGFP (X4 HIV) were applied to the surface of abraded skin explants, and emigrant cells were cocultured with allogeneic T cells. Twelve days following coculture, GFP^+ cells were observed from $NLCSF_{V3}EGFP$ or JRFLEGFP infections, but not from NL43EGFP infections (data not shown). To quantify numbers of HIV-transmitted T cells at the single-cell level, emigrating cells were labeled with PKH67 Red before coculture with T cells and then analyzed by flow cytometry. When $NLCSF_{V3}EGFP$ or JRFLEGFP was applied to skin, a few $GFP^+PKH^-CD3^+$ T cells (R2) as well as PKH^+ skin emigrants (R1) were detected (Fig. 6). By contrast, when NL43EGFP or heat-inactivated $NLCSF_{V3}EGFP$ was applied to skin, GFP^+ cells were <0.2% in both fractions (Fig. 6). Consistent with CCR5-dependent virus dissemination in this model (Fig. 1), these findings indicate that LC are preferentially infected with R5 HIV and transmit virus to cocultured T cells, most likely because of differential cell surface expression of CCR5 and CXCR4 on LC (25, 35).

Discussion

Percutaneous injury, usually inflicted by a hollow-bore needle, is the most common route of occupational HIV transmission. HIV may be transmitted to an accident victim by direct inoculation of exogenous virus into recipient blood vessels of the dermis. In addition, our results suggest that DC subsets that are resident within skin may also play a role in initial infection and dissemination of virus. There could be several possible pathways that HIV is transmitted from resident cutaneous DC to T cells, as follows: de novo or *cis* infection-dependent pathway or infection-independent pathways via CLR (37–39). Following spontaneous epidermal and dermal exposure, we found that transmission of HIV from skin emigrants to T cells occurs through a CD4- and a CLR-dependent manner. Blockade of CD4 substantially inhibited subsequent HIV dissemination, whereas blockade of CLR partially inhibited virus dissemination (Fig. 1). In addition, combination of CD4 and CLR blockade did not increase inhibition provided by CD4 mAb alone, suggesting that de novo infection is predominantly involved in the uptake of virus by resident skin DC. Of note is that, although HIV dissemination by migratory cells is largely mediated by DC subsets, T cells within migratory cells also contributed partially. This suggests that DC-T cell conjugates contribute greatly to viral dissemination, as suggested by previous findings that HIV infection is highest in DC-T cell conjugates when emigrated skin cells were directly exposed to HIV (33, 40).

The molecular and cellular events that occur following occupational exposure of nonintact skin to HIV have not been previously defined. Our data indicate that CD4- and CCR5-mediated productive HIV infection of LC, and not C-type lectin-mediated capture of virus by LC or DC, play a major role in virus dissemination when the epidermal surface of abraded skin is exposed to virus. Selective infection of epidermal LC within skin resident DC populations observed in our model may be due to restricted access to subepithelial cells conferred by desmosomes and tight junctions within epithelial tissue (38).

Reece et al. (31) also used skin explants to model early events of HIV transmission. These investigators exposed HIV to skin specimens overnight, and, using a PCR-based assay, demonstrated that R5 HIV was found in both epidermal and dermal emigrant DC. The conflicting findings regarding infection of dermal DC may be a result of the duration of virus exposure to the epidermal surface of abraded skin (overnight vs 2 h). Because similar conflicting results were observed in the rhesus macaques studies (12–14), it is probable that virus-infected LC emigrate from epithelial surfaces into subepithelial tissues during overnight virus exposure. Thus, our data suggest that epithelial LC play a critical early role in transmitting R5 HIV to cells within underlying subepithelial tissue.

Unlike effective R5 HIV dissemination by LC, LC emigrating from X4 HIV-exposed skin explants failed to transmit infection to cocultured T cells (Fig. 6). In cocultures, R5 viral infection in LC was much more efficient than X4 virus infection (Figs. 5 and 6), suggesting LC are preferentially infected with R5 HIV probably due to differential HIV coreceptor expression on resident LC (25). In this regard, it has been reported that DC-SIGN, and probably other CLR (including langerin), bind R5 and X4 viruses equally well (16), suggesting that these molecules may not be responsible for the preferential selection of R5 viruses observed in our model. By contrast, a recent study revealed that langerin on LC prevents LC infection of HIV and viral dissemination (41). This study showed that HIV captured by langerin was internalized into Birbeck granules and degraded. Nevertheless, our results indicate that when LC were exposed to HIV at high virus concentrations (10,000 TCID), significant LC infection of R5 virus and viral transmission to T cells were observed, suggesting that langerin is saturated at these concentrations and is not able to protect against infection. Because CCR5-dependent and CLR-independent virus dissemination was predominantly observed in our model using high concentrations of R5 HIV (Fig. 2), we believe that direct HIV infection of resident LC most likely plays a pivotal role in occupational transmission of HIV following exposure of nonintact skin. The disruption of the corneal layer of the epidermis before virus application to the surface of skin was necessary for LC infection of HIV, indicating that the corneal layer functions as a protective barrier for intact skin. Alternatively, it is possible the abrasion of skin might induce LC activation and subsequent down-regulation of langerin, leading to the enhanced infection of LC in our model.

Furthermore, HIV replication in cocultures predominantly occurred in LC-T cell conjugates (Fig. 5). Because activated CD34-derived LC have been recently shown to facilitate the *trans* infection of cocultured T cells (42), LC-T cell conjugates may allow for T cell-mediated activation of LC and subsequent *trans* infection from HIV-infected LC to responding T cells.

In the retrospective case-control study of HCP, use of zidovudine as postexposure prophylaxis (PEP) was associated with a reduction in the risk of HIV infection (43). Animal studies have demonstrated the importance of starting PEP soon after an exposure (44, 45), and PEP probably is substantially less effective when started >24–36 h postexposure (45, 46). In addition, larger viral inoculates decreased prophylactic efficacy (47, 48). Our data support the importance of starting PEP soon after an exposure, because PEP may prevent systemic infection and larger viral production of T cells. Because LC most likely become infected soon after exposure, PEP is probably not acting upon HIV replication in these cells, but rather the later step of LC-mediated infection of T cells. In addition to the timing of starting PEP, our findings suggest that other factors (e.g., presence of R5 HIV strains in the source person) may influence the efficacy of PEP. Further studies are now underway using our model to determine the effects of PEP administered at various times following HIV exposure.

Acknowledgments

We thank Naoki Yamamoto, Naotaka Shibagaki, and Hiroyuki Matsue for helpful discussions, and Izumi Ishikawa for technical assistance.

Disclosures

The authors have no financial conflict of interest.

References

1. Updated US Public Health Service guidelines on the management of occupational exposures to HBV, HCV, and HIV and recommendations for post-exposure prophylaxis. 2001. *Morbid. Mortal. Wkly. Rep.* 50(RR-11): 1–67.
2. Bell, D. M. 1997. Occupational risk of human immunodeficiency virus infection in healthcare workers: an overview. *Am. J. Med.* 102: 9–15.
3. CDC. 1987. Update: human immunodeficiency virus infections in health-care workers exposed to blood of infected patients. *Morbid. Mortal. Wkly. Rep.* 36: 285–289.
4. Liu, R., W. A. Paxton, S. Choe, D. Ceradini, S. R. Martin, R. Horuk, M. E. MacDonald, H. Stuhlmann, R. A. Koup, and N. R. Landau. 1996. Homozygous defect in HIV-1 coreceptor accounts for resistance of some multiply-exposed individuals to HIV-1 infection. *Cell* 86: 367–377.
5. Dean, M., M. Carrington, C. Winkler, G. A. Huttley, M. W. Smith, R. Allikmets, J. J. Goedert, S. P. Buchbinder, E. Vittinghoff, E. Gomperts, et al. 1996. Genetic restriction of HIV-1 infection and progression to AIDS by a deletion allele of the CKR5 structural gene. *Science* 273: 1856–1862.
6. Samson, M., F. Libert, B. J. Doranz, J. Rucker, C. Liesnard, C. M. Farber, S. Saragosti, C. Lapoumeroulie, J. Cognaux, C. Forceille, et al. 1996. Resistance to HIV-1 infection in Caucasian individuals bearing mutant alleles of the CCR-5 chemokine receptor gene. *Nature* 382: 722–725.
7. Huang, Y., W. A. Paxton, S. M. Wolinsky, A. U. Neumann, L. Zhang, T. He, S. Kang, D. Ceradini, Z. Jin, K. Yazdanbakhsh, et al. 1996. The role of a mutant CCR5 allele in HIV-1 transmission and disease progression. *Nat. Med.* 2: 1240–1243.
8. Zhang, L. Q., P. MacKenzie, A. Cleland, E. C. H. J. Brown, and P. Simmonds. 1993. Selection for specific sequences in the external envelope protein of human immunodeficiency virus type 1 upon primary infection. *J. Virol.* 67: 3345–3356.
9. Zhu, T., H. Mo, N. Wang, D. S. Nam, Y. Cao, R. A. Koup, and D. D. Ho. 1993. Genotypic and phenotypic characterization of HIV-1 patients with primary infection. *Science* 261: 1179–1181.
10. Van't Wout, A. B., N. A. Kootstra, G. A. Mulder-Kampinga, N. Albrecht-van Lent, H. J. Scherpbier, J. Veenstra, K. Boer, R. A. Coutinho, F. Miedema, and H. Schuitemaker. 1994. Macrophage-tropic variants initiate human immunodeficiency virus type 1 infection after sexual, parenteral, and vertical transmission. *J. Clin. Invest.* 94: 2060–2067.
11. Lederman, M. M., R. S. Veazey, R. Offord, D. E. Mosier, J. Dufour, M. Mefford, M. Piatak, Jr., J. D. Lifson, J. R. Salkowitz, B. Rodriguez, et al. 2004. Prevention of vaginal SHIV transmission in rhesus macaques through inhibition of CCR5. *Science* 306: 485–487.
12. Zhang, Z. Q., T. Schuler, M. Zupancic, S. Wietgrefe, K. A. Staskus, K. A. Reimann, T. A. Reinhart, M. Rogan, W. Cavert, C. J. Miller, et al. 1999. Sexual transmission and propagation of SIV and HIV in resting and activated CD4$^+$ T cells. *Science* 286: 1353–1357.
13. Spira, A. I., P. A. Marx, B. K. Patterson, J. Mahoney, R. A. Koup, S. M. Wolinsky, and D. D. Ho. 1996. Cellular targets of infection and route of viral dissemination after an intravaginal inoculation of simian immunodeficiency virus into rhesus macaques. *J. Exp. Med.* 183: 215–225.
14. Hu, J., M. B. Gardner, and C. J. Miller. 2000. Simian immunodeficiency virus rapidly penetrates the cervicovaginal mucosa after intravaginal inoculation and infects intraepithelial dendritic cells. *J. Virol.* 74: 6087–6095.
15. Krutzik, S. R., B. Tan, H. Li, M. T. Ochoa, P. T. Liu, S. E. Sharfstein, T. G. Graeber, P. A. Sieling, Y. J. Liu, T. H. Rea, et al. 2005. TLR activation triggers the rapid differentiation of monocytes into macrophages and dendritic cells. *Nat. Med.* 11: 653–660.
16. Geijtenbeek, T. B., D. S. Kwon, R. Torensma, S. J. van Vliet, G. C. van Duijnhoven, J. Middel, I. L. Cornelissen, H. S. Nottet, V. N. KewalRamani, D. R. Littman, et al. 2000. DC-SIGN, a dendritic cell-specific HIV-1-binding protein that enhances *trans*-infection of T cells. *Cell* 100: 587–597.
17. Kwon, D. S., G. Gregorio, N. Bitton, W. A. Hendrickson, and D. R. Littman. 2002. DC-SIGN-mediated internalization of HIV is required for *trans*-enhancement of T cell infection. *Immunity* 16: 135–144.
18. Granelli-Piperno, A., A. Pritsker, M. Pack, I. Shimeliovich, J. F. Arrighi, C. G. Park, C. Trumpfheller, V. Piguet, T. M. Moran, and R. M. Steinman. 2005. Dendritic cell-specific intercellular adhesion molecule 3-grabbing nonintegrin/CD209 is abundant on macrophages in the normal human lymph node and is not required for dendritic cell stimulation of the mixed leukocyte reaction. *J. Immunol.* 175: 4265–4273.
19. Burleigh, L., P. Y. Lozach, C. Schiffer, I. Staropoli, V. Pezo, F. Porrot, B. Canque, J. L. Virelizier, F. Arenzana-Seisdedos, and A. Amara. 2006. Infection of dendritic cells (DCs), not DC-SIGN-mediated internalization of human immunodeficiency virus, is required for long-term transfer of virus to T cells. *J. Virol.* 80: 2949–2957.
20. Turville, S. G., P. U. Cameron, A. Handley, G. Lin, S. Pohlmann, R. W. Doms, and A. L. Cunningham. 2002. Diversity of receptors binding HIV on dendritic cell subsets. *Nat. Immunol.* 3: 975–983.
21. Lee, B., G. Leslie, E. Soilleux, U. O'Doherty, S. Baik, E. Levroney, K. Flummerfelt, W. Swiggard, N. Coleman, M. Malim, and R. W. Doms. 2001. *cis* Expression of DC-SIGN allows for more efficient entry of human and simian immunodeficiency viruses via CD4 and a coreceptor. *J. Virol.* 75: 12028–12038.
22. Kawamura, T., S. S. Cohen, D. L. Borris, E. A. Aquilino, S. Glushakova, L. B. Margolis, J. M. Orenstein, R. E. Offord, A. R. Neurath, and A. Blauvelt. 2000. Candidate microbicides block HIV-1 infection of human immature Langerhans cells within epithelial tissue explants. *J. Exp. Med.* 192: 1491–1500.
23. Kawamura, T., F. O. Gulden, M. Sugaya, D. T. McNamara, D. L. Borris, M. M. Lederman, J. M. Orenstein, P. A. Zimmerman, and A. Blauvelt. 2003. R5 HIV productively infects Langerhans cells, and infection levels are regulated by compound CCR5 polymorphisms. *Proc. Natl. Acad. Sci. USA* 100: 8401–8406.
24. Kawamura, T., S. E. Bruse, A. Abraha, M. Sugaya, O. Hartley, R. E. Offord, E. J. Arts, P. A. Zimmerman, and A. Blauvelt. 2004. PSC-RANTES blocks R5 human immunodeficiency virus infection of Langerhans cells isolated from individuals with a variety of CCR5 diplotypes. *J. Virol.* 78: 7602–7609.
25. Zaitseva, M., A. Blauvelt, S. Lee, C. K. Lapham, V. Klaus-Kovtun, H. Mostowski, J. Manischewitz, and H. Golding. 1997. Expression and function of CCR5 and CXCR4 on human Langerhans cells and macrophages: implications for HIV primary infection. *Nat. Med.* 3: 1369–1375.
26. Simmons, G., P. R. Clapham, L. Picard, R. E. Offord, M. M. Rosenkilde, T. W. Schwartz, R. Buser, T. N. C. Wells, and A. E. Proudfoot. 1997. Potent inhibition of HIV-1 infectivity in macrophages and lymphocytes by a novel CCR5 antagonist. *Science* 276: 276–279.
27. Ichiyama, K., S. Yokoyama-Kumakura, Y. Tanaka, R. Tanaka, K. Hirose, K. Bannai, T. Edamatsu, M. Yanaka, Y. Niitani, N. Miyano-Kurosaki, et al. 2003. A duodenally absorbable CXC chemokine receptor 4 antagonist, KRH-1636, exhibits a potent and selective anti-HIV-1 activity. *Proc. Natl. Acad. Sci. USA* 100: 4185–4190.
28. Koyanagi, Y., S. Miles, R. T. Mitsuyasu, J. E. Merrill, H. V. Vinters, and I. S. Chen. 1987. Dual infection of the central nervous system by AIDS viruses with distinct cellular tropisms. *Science* 236: 819–822.
29. Miura, Y., N. Misawa, Y. Kawano, H. Okada, Y. Inagaki, N. Yamamoto, M. Ito, H. Yagita, K. Okumura, H. Mizusawa, and Y. Koyanagi. 2003. Tumor necrosis factor-related apoptosis-inducing ligand induces neuronal death in a murine model of HIV central nervous system infection. *Proc. Natl. Acad. Sci. USA* 100: 2777–2782.
30. Collins, K. B., B. K. Patterson, G. J. Naus, D. V. Landers, and P. Gupta. 2000. Development of an in vitro organ culture model to study transmission of HIV-1 in the female genital tract. *Nat. Med.* 6: 475–479.
31. Reece, J. C., A. J. Handley, E. J. Anstee, W. A. Morrison, S. M. Crowe, and P. U. Cameron. 1998. HIV-1 selection by epidermal dendritic cells during transmission across human skin. *J. Exp. Med.* 187: 1623–1631.
32. Lenz, A., M. Heine, G. Schuler, and N. Romani. 1993. Human and murine dermis contain dendritic cells: isolation by means of a novel method and phenotypical and functional characterization. *J. Clin. Invest.* 92: 2587–2596.
33. Pope, M., S. Gezelter, N. Gallo, L. Hoffman, and R. M. Steinman. 1995. Low levels of HIV-1 infection in cutaneous dendritic cells promote extensive viral replication upon binding to memory CD4$^+$ T cells. *J. Exp. Med.* 182: 2045–2056.
34. Ball, S. C., A. Abraha, K. R. Collins, A. J. Marozsan, H. Baird, M. E. Quinones-Mateu, A. Penn-Nicholson, M. Murray, N. Richard, M. Lobritz, et al. 2003. Comparing the ex vivo fitness of CCR5-tropic human immunodeficiency virus type 1 isolates of subtypes B and C. *J. Virol.* 77: 1021–1038.

35. Kawamura, T., M. Qualbani, E. K. Thomas, J. M. Orenstein, and A. Blauvelt. 2001. Low levels of productive HIV infection in Langerhans cell-like dendritic cells differentiated in the presence of TGF-β1 and increased viral replication with CD40 ligand-induced maturation. *Eur. J. Immunol.* 31: 360–368.
36. Sugaya, M., K. Lore, R. A. Koup, D. C. Douek, and A. Blauvelt. 2004. HIV-infected Langerhans cells preferentially transmit virus to proliferating autologous $CD4^+$ memory T cells located within Langerhans cell-T cell clusters. *J. Immunol.* 172: 2219–2224.
37. Miller, C. J., and R. J. Shattock. 2003. Target cells in vaginal HIV transmission. *Microbes Infect.* 5: 59–67.
38. Shattock, R. J., and J. P. Moore. 2003. Inhibiting sexual transmission of HIV-1 infection. *Nat. Rev. Microbiol.* 1: 25–34.
39. Kawamura, T., S. E. Kurtz, A. Blauvelt, and S. Shimada. 2005. The role of Langerhans cells in the sexual transmission of HIV. *J. Dermatol. Sci.* 40: 147–155.
40. Pope, M., M. G. H. Betjes, N. Romani, P. U. Cameron, L. Hoffman, S. Gezelter, G. Schuler, and R. M. Steinman. 1994. Conjugates of dendritic cells and memory T lymphocytes from skin facilitate productive infection with HIV-1. *Cell* 78: 389–398.
41. De Witte, L., A. Nabatov, M. Pion, D. Fluitsma, M. A. de Jong, T. de Gruijl, V. Piguet, Y. van Kooyk, and T. B. Geijtenbeek. 2007. Langerin is a natural barrier to HIV-1 transmission by Langerhans cells. *Nat. Med.* 13: 367–371.
42. Fahrbach, K. M., S. M. Barry, S. Ayehunie, S. Lamore, M. Klausner, and T. J. Hope. 2007. Activated CD34-derived Langerhans cells mediate transinfection with human immunodeficiency virus. *J. Virol.* 81: 6858–6868.
43. Cardo, D. M., D. H. Culver, C. A. Ciesielski, P. U. Srivastava, R. Marcus, D. Abiteboul, J. Heptonstall, G. Ippolito, F. Lot, P. S. McKibben, and D. M. Bell. 1997. A case-control study of HIV seroconversion in health care workers after percutaneous exposure: Centers for Disease Control and Prevention Needlestick Surveillance Group. *N. Engl. J. Med.* 337: 1485–1490.
44. Martin, L. N., M. Murphey-Corb, K. F. Soike, B. Davison-Fairburn, and G. B. Baskin. 1993. Effects of initiation of 3'-azido,3'-deoxythymidine (zidovudine) treatment at different times after infection of rhesus monkeys with simian immunodeficiency virus. *J. Infect. Dis.* 168: 825–835.
45. Bottiger, D., N. G. Johansson, B. Samuelsson, H. Zhang, P. Putkonen, L. Vrang, and B. Oberg. 1997. Prevention of simian immunodeficiency virus, SIVsm, or HIV-2 infection in cynomolgus monkeys by pre- and postexposure administration of BEA-005. *AIDS* 11: 157–162.
46. Tsai, C. C., K. E. Follis, A. Sabo, T. W. Beck, R. F. Grant, N. Bischofberger, R. E. Benveniste, and R. Black. 1995. Prevention of SIV infection in macaques by (R)-9-(2-phosphonylmethoxypropyl)adenine. *Science* 270: 1197–1199.
47. Sinet, M., B. Desforges, O. Launay, J. N. Colin, and J. J. Pocidalo. 1991. Factors influencing zidovudine efficacy when administered at early stages of Friend virus infection in mice. *Antiviral Res.* 16: 163–171.
48. Fazely, F., W. A. Haseltine, R. F. Rodger, and R. M. Ruprecht. 1991. Post-exposure chemoprophylaxis with ZDV or ZDV combined with interferon-α: failure after inoculating rhesus monkeys with a high dose of SIV. *J. Acquired Immune Defic. Syndr.* 4: 1093–1097.

Journal of Medical Virology 80:1322–1331 (2008)

A Novel CD4-Conjugated Ultraviolet Light-Activated Photocatalyst Inactivates HIV-1 and SIV Efficiently

Koushi Yamaguchi,[1,2]* Takahiro Sugiyama,[2,3] Shinji Kato,[3] Yoichi Kondo,[3] Naohide Ageyama,[4] Masaru Kanekiyo,[2] Misao Iwata,[3] Yoshio Koyanagi,[5] Naoki Yamamoto,[2] and Mitsuo Honda[6]

[1]*Department of Perinatology, National Center for Child Health and Development, Setagaya-ku, Tokyo, Japan*
[2]*AIDS Research Center, National Institute of Infectious Diseases, Shinjuku-ku, Tokyo, Japan*
[3]*Research and Development Center, Noritake Co., Nishi-ku, Nagoya, Japan*
[4]*Tsukuba Primate Research Center, National Institute of Biomedical Innovation, Tsukuba-shi, Ibaraki, Japan*
[5]*Institute for Virus Research, Kyoto University, Kawahara-cho, Shogoin, Sakyo-ku, Kyoto, Japan*
[6]*Vaccine Research Center, National Institute of Allergy and Infectious Diseases, National Institutes of Health, Bethesda, Maryland*

In this study, we found that the electric potential derived from the redox reaction of ultraviolet (UV)-illuminated CD4-conjugated titanium dioxide (TiO_2) inactivated a wide range of high-titered primary HIV-1 isolates, regardless of virus co-receptor usage or genetic clade. In vitro incubation of HIV-1 isolates with CD4-conjugated TiO_2 (CD4-TiO_2) followed by UV illumination led to inhibition of viral infectivity in both H9 cells and peripheral blood mononuclear cells as well as to the complete inactivation of plasma virions from HIV-1-infected individuals. Treatment with a newly established extra-corporeal circulation system with the photocatalyst in rhesus macaques completely inactivated plasma virus in the system and effectively reduced the infectious plasma viral load. Furthermore, plasma viremia and infectious viral loads were controlled following a second therapeutic photocatalyst treatment during primary SIV_{mac239} infection of macaques. Our findings suggest that this therapeutic immunophysical strategy may help control human immunodeficiency viral infection in vivo. ***J. Med. Virol. 80:1322–1331, 2008.*** © 2008 Wiley-Liss, Inc.

KEY WORDS: ultraviolet light; photocatalyst; CD4-conjugated TiO_2; HIV; SIV

INTRODUCTION

Novel strategies for cross-neutralizing or inactivating a broad spectrum of primary HIV-1 strains are currently of vital interest [Pantaleo and Koup, 2004; Robinson and Amara, 2005]. In this article, we report on a new strategy for the inactivation of primary HIV-1 isolates using CD4 peptides bound to the surface of TiO_2 together with exposure to the electric potential generated by UV illumination of TiO_2. TiO_2 is a relatively benign inorganic compound that can be activated by UV. The irradiated TiO_2 causes the formation of an electron hole (electron: e^-; hole: h^+) pair on the surface and leads to redox reactions with all organic matter at the surface of the TiO_2, resulting in the production of CO_2 and O_2 (Fig. 1A). The energy of the free radicals from TiO_2 in water is predominantly pro-oxidative, with a hydrogen electric potential standard of approximately +3.2 V. That potential is recognized as being extremely high when compared to that of other oxidants, such as chlorine (+1.36 V) or ozone (+2.07 V) [Fujishima and Honda, 1972; Ishibashi et al., 1998]. The effects are only observed on the surface of TiO_2, leaving unaffected molecules which are not in contact with the surface. Thus, TiO_2 has no toxicity itself and is activated only when illuminated by UV, meaning that it is harmless to and cannot be activated in the human body. Specific binding of HIV-1 on the surface of CD4-conjugated TiO_2 resulted in efficient virus inactivation effects and suggested the possibility of obtaining greater therapeutic selectivity for a given clinical application.

MATERIALS AND METHODS

Animals and SIV Challenge

Macaques of Myanmar origin were purchased from Japan SLC [Someya et al., 2005]. Three male rhesus

The authors have no conflicting financial interest.

*Correspondence to: Dr. Koushi Yamaguchi, MD, PhD, Division of Maternal Medicine, Department of Perinatology, National Center for Child Health and Development, Okura 2-10-1, Setagaya-ku, Tokyo 157-8535, Japan.
E-mail: yamaguchi-k@ncchd.go.jp

Accepted 22 April 2008
DOI 10.1002/jmv.21235
Published online in Wiley InterScience (www.interscience.wiley.com)

macaques (*Macaca mulatta*; R27, R28, and R29) were used for the evaluation of the photocatalyst treatment, with another five macaques used as controls [Someya et al., 2005]. Before use, these macaques were tested and found to be negative for SeV, SIV, and simian retrovirus type D. All animals were housed in individual cages and maintained in accordance with the rules and guidelines for experimental animal welfare set forth by the National Institute of Infectious Diseases and National Institute of Biomedical Innovation in Japan. SIV_{mac239} was kindly provided by Dr. Kazuyasu Mori, AIDS Research Center, National Institute of Infectious Diseases, Tokyo, Japan. The virus obtained from COS1 cells transfected with SIV_{mac239} molecular clone pBRmac239 was propagated in rhesus macaque PBMCs to prepare the challenge stock [Kestler et al., 1991]. The study was performed in the P3 facility following guidelines established by the laboratory biosafety manual of the World Health Organization [Someya et al., 2005]. Rhesus macaques were infected intravenously with 1,000 $TCID_{50}$ of SIV_{mac239} [Matano et al., 2004], with treatment using the extra-corporeal circulation system performed on day 10 post-infection, as described below.

Study of Human Subjects

All six blood samples from individuals seropositive for HIV-1 were collected through the Committee for Collaborative HIV Study of the National Cooperative Preventive Study Group for AIDS in Japan. The study on human subjects was approved by the Institutional Review Board of each study-related institution in Japan.

Virus and Sera From HIV-Infected Individuals

The primary clinical isolate $HIV\text{-}1_{MNp}$ was kindly provided by Dr. J. Sullivan of the University of Massachusetts Medical School, MA, USA. The virus was confirmed to be resistant to neutralization by Dr. S. Zolla-Pazner of the New York University School of Medicine, NY, USA [Cecilia et al., 1998; Matano et al., 2004]. Laboratory-adapted $HIV\text{-}1_{89.6}$ and $HIV\text{-}1_{MN}$ were obtained from the AIDS Research and Reference Reagent Program, National Institutes of Health, MD, USA. $HIV\text{-}1_{MN}$ (H9/HTLV-III MN, AIDS Research and Reference Reagent Program) and $HIV\text{-}1_{IIIB}$ (H9/HTLV-IIIB NIH1983, AIDS Research and Reference Reagent Program) were propagated in PBMC [Ye et al., 2000]. The WHO primary isolates 92TH002, 92TH022, 92TH023 (clade E), and 92TH014 (clade B′) were used as undiluted virus stocks [Honda et al., 1995]. The primary isolates $HIV\text{-}1_{JR\text{-}CSF}$, $HIV\text{-}1_{JR\text{-}FL}$, and the CS and JCI series of HIV-1 isolates were provided by Koyanagi et al. [1987] and Okamoto et al. [1998]. Sera were obtained from HIV-1-infected Japanese patients who had been sero-positive for more than 1 year (HIV-1 specimen bank, AIDS Research Center, National Institute of Infectious Diseases, Tokyo, Japan) [Nakasone et al., 2000] and from healthy controls.

A CD4-Conjugated Photocatalyst and Adsorption of HIV Virions

The anatase form of the TiO_2 particle (size: 0.5 μm in diameter) was used as a photocatalyst. For conjugation of CD4, TiO_2 was incubated with 0–10% 3-aminopropyl trimethoxysilane (APTMS; Tokyo Kasei Kogyo) in hexane at 80°C. The TiO_2 was rinsed twice with 100% methyl alcohol and phosphate-buffered saline (PBS) before being incubated with 3% glutaraldehyde in PBS at room temperature for 30 min. After being washed twice with PBS, the cross-linker-immobilized TiO_2 was incubated with 10 μg/ml of CD4 ($[Cys(Bzl)]^{84}$-Fragment 81-92, Sigma Chemical Co., St. Louis, MO) in PBS at 4°C. To physically remove non-adsorbed CD4, the TiO_2 was rinsed twice with 2.0 M sodium chloride solution and immersed in PBS until use.

The surface of CD4-conjugated TiO_2 was scanned by AFM (Nanoscope III, Veeco, Santa Barbara, CA). CD4-conjugated or non-conjugated TiO_2 was incubated with $HIV\text{-}1_{IIIB}$ (100 ng/ml of p24 antigen) in RPMI for 1 hr at 37°C and then washed twice with PBS to remove non-adsorbed virions. The virus-treated TiO_2 was dehydrated, coated with platinum, and scanned using SEM (JSM-6301F, JEOL, Tokyo, Japan) according to the manufacturer's instructions.

H9- and PBMC-Based Virus Infectivity Assays

Using H9 (HUT78) cells provided by Dr. R. Gallo [Gazdar et al., 1980] as targets of infection, the T cell line-adapted (TCLA) strain $HIV\text{-}1_{IIIB}$ was inactivated by treatment with TiO_2. Five hundred microliters of serially diluted $HIV\text{-}1_{IIIB}$ were incubated with the indicated concentrations of either TiO_2 or CD4-TiO_2 in 24-well plates (Corning, Corning, NY) under indicated intensities of UV illumination with gentle shaking. The UV was generated by a 10-watt black light fluorescent lamp (wavelength 300–400 nm, peak 360 nm, near-UV light including visible blue light) and the light intensity was measured in the center of the vessel with a UV radiometer (UM-10: receptor head UM-360, Konica Minolta, Osaka, Japan).

After the indicated duration of illumination, the virus solution was filtered with a 0.45-μm pore size cellulose acetate hydrophilic filter (ADVANTEC Toyo, Tokyo, Japan) to remove TiO_2 or CD4-TiO_2 and then incubated with H9 cells at a concentration of 4×10^5 cells in 500 μl of RPMI medium for 1 hr at 37°C. To remove the input virus inoculum, the medium was replaced by centrifugation three times and 4×10^4 cells in 200 μl were cultured in 96-well plates for 5 days post-infection. The amount of HIV-1 p24 antigen was then measured in the culture supernatants using Lumipulse I HIV-1 p24 chemiluminescent enzyme-automated immunoassay (CLEIA; Fujirebio Co., Tokyo, Japan).

The effect of inactivation of primary HIV-1 isolates and $HIV\text{-}1_{IIIB}$ on infection of mitogen-activated PBMC was determined essentially as previously described [Honda et al., 1992; Conley et al., 1994; Weber et al., 1996; Chujoh et al., 2001]. The $TCID_{50}$ for all virus

stocks was determined in advance using PBMC batched for use in these and all subsequent infectivity assays. This batch of PBMC was selected from fresh peripheral cells collected at the Japanese Red Cross Blood Center, Japanese Red Cross Society, Tokyo, Japan on the basis of the high infectivity of HIV-1_{JRCSF} and HIV-1_{MN_P}. Briefly, 500 $TCID_{50}$ of either virus stock or patient plasma was treated with 0.25% (w/v) CD4-TiO_2 in 500 μl at 60 min UV illumination for 0.8 mW/cm^2. The treated virus solution (150 μl) was filtered and then combined with 75 μl of complete RPMI containing 10^5 PHA-activated PBMC in 96-well plates. To remove the input inoculum, the medium was replaced three times over the following 3 days, and the culture was continued for 7 days post-infection, after which time the amount of HIV-1 p24 in the medium was measured.

Determination of HIV-1 Proviral DNA by PCR

HIV-1 treated with TiO_2 (500 μl) and UV illumination or control preparations were mixed with H9 cells at a concentration of 8×10^5 cells/ml in 500 μl of complete RPMI medium. After incubation for 48 hr at 37°C in 5% CO_2, the cells were harvested for DNA extraction. HIV-1 proviral DNA was amplified from cell lysates by polymerase chain reaction (PCR) using SK68 and SK69 primers encompassing the HIV-1 *env* gene, as previously described [Ou et al., 1988; Zimmerman et al., 1996].

Quantitative Analysis of Infectious Virus Using MAGIC-5 Assay

MAGIC-5 cells were derived from HeLa-CD4-LTR-β-gal (MAGI) cells and express both CD4 and CCR5 receptors [Hachiya et al., 2001]. Cells were maintained in D-MEM (GibcoBRL, Long Island, NY) complete medium (5% heat-inactivated fetal bovine serum, 100 units/ml penicillin, 100 μg/ml streptomycin, 2 mM L-glutamine, and 25 mM HEPES buffer) supplemented with 0.2 mg/ml G148 (Sigma), 50 units/ml hygromycin (Sigma) and 1 μg/ml blasticidin S (Funakoshi Co., Tokyo, Japan) at 37°C in 5% CO_2. MAGIC-5 cells were plated in 98-well plates (Corning) at 4×10^4 cells per well in 100 μl of complete D-MEM medium the day before infection. The medium was removed from each well, and 100 μl of the treated virus solution was added and then incubated for 3 days at 37°C in a 5% CO_2 incubator. After incubation, the medium containing virus was removed, and the cells were fixed in 50 μl of fixation solution (1% formaldehyde, 0.2% glutaraldehyde in PBS) for 5 min and then washed well with PBS. The fixed cells were incubated with 100 μl of staining solution [4 mM potassium ferrocyanide, 4 mM potassium ferricyanide, 2 mM $MgCl_2$ and 0.4 mg/ml X-gal (5-bromo-4-chloro-3-indolyl β-D-galactopyranoside, Sigma) in PBS] for 60 min at 37°C. The staining was stopped by removing the staining solution and washing twice with PBS. The numbers of blue-stained infected cells in each well were counted manually by microscopic observation.

Comparison of the Adsorptive and Photocatalytic Effects of CD4-Conjugated TiO_2

CD4-conjugated TiO_2 was prepared using the indicated concentrations of APTMS. CD4-conjugated TiO_2 at a concentration of 0.25% (w/v) was incubated with HIV-1_{IIIB} (100 ng/ml of p24 antigen) in 500 μl of complete medium for 30 min, with or without UV illumination (0.8 mW/cm^2) under gentle shaking at 37°C, and then filtered. The amount of HIV-1 p24 antigen in the non-UV illuminated medium was measured and UV illuminated medium was used for H9-based virus infectivity assays, to estimate un-adsorbed viruses after adsorption and residual infectious viruses after photocatalysis with adsorption.

In Vitro Inactivation of SIV_{mac239}

Using GHOST-R5 cells kindly provided by Dr. Susan Zolla-Pazner, New York University School of Medicine, New York, NY as targets of infection [Someya et al., 2005], SIV_{mac239} was inactivated by treatment with UV-illuminated TiO_2. Five hundred microliters of normal human plasma containing 30 ng/ml of SIV_{mac239} were incubated with the 2.0% (w/v) of either TiO_2 or CD4-TiO_2 in 24-well plates (Corning) under UV illumination with gentle shaking. After 30 min of incubation, the virus-containing plasma was filtered to remove TiO_2 or CD4-TiO_2 and then incubated with the monolayers of GHOST cells, about 70% confluent at 37°C. On the following day, virus-containing plasma was removed and the cell monolayers were washed once with PBS. Subsequently, 1 ml of complete medium was added per well. The day on which the virus was added was considered day 0. On day 4, cells were harvested, once again washed with PBS, resuspended in 300 ml of 1 mM EDTA in PBS, and fixed in formaldehyde at a final concentration of 2%. The cells were then analyzed with a FACScan flow cytometer (Becton Dickinson Co., Franklin Lakes, NJ). The live cells were gated on the basis of forward and side scatter. The number of infected cells was determined using a scattergram of fluorescence versus forward scatter after setting the gates with uninfected cells. A total of 15,000–20,000 events were scored.

Extra-Corporeal Circulation

The extra-corporeal circulation system devised for UV-illuminated CD4-TiO_2 treatment was equipped with a CS3000 blood cell separator (Baxter) to separate plasma, a CD4-TiO_2 circulatory system with UV illumination, and a plasma separation filter (Fig. 3B). Sequential plasma separation from whole blood using the CS3000 was performed by centrifugation, and circuit and circulation protocols were modified and applied to rhesus monkeys [Donahue et al., 1996; Ageyama et al., 2003]. The plasma separation system was synchronized to the CD4-TiO_2 circulatory system, with a blood flow rate of 8–12 ml/min and a plasma flow rate of 100 ml/min in the circulatory system of

CD4-TiO_2. The flow rate of separated plasma in and out of the CD4-TiO_2 circulatory system was approximately 4–6 ml/min. The final concentration of 10% ACD-A (an acid citrate dextrose-A) solution was used as an anticoagulant. The plasma mixed with CD4-TiO_2 in a part of the circulatory system was then subjected to UV illumination. The CD4-TiO_2 particles were separated by filter and left in the circulatory system. The treated plasma, now CD4-TiO_2 particle-free, was sequentially separated from the circulatory system, put back into the blood cell separator, and mixed with separated blood cells before being returned to the monkey. Before starting the treatment, the extracorporeal circuit was primed with autologous blood collected 3 weeks before the treatment. The draw line and inlet return were taken from the femoral artery and saphenous vein, respectively, and the total throughput, 2–2.5 times the estimated total blood volume of each animal, was treated for approximately 1.5–2 hr. Twenty minutes after initiation, plasma collection for analysis was started at the inlet and outlet of the circulatory CD4-TiO_2 system. All procedures were performed under general anesthesia (A.D.S.1000; Shin-ei) with isoflurane gas. Vital signs were monitored with electrocardiography, blood pressure, oxygen saturation and respiration.

Quantitation of Infectious Virus Titers in Plasma

Plasma (20 μl) was incubated with M8166 cells [Honda et al., 1992] at a concentration of 8×10^4 cells in 20 μl of RPMI medium for 1 hr at 37°C. To remove the input plasma, the cells were washed three times with PBS and 8×10^4 cells in 200 μl were cultured in 96-well plates for 4 days post-infection. SIV p27 antigen produced from infected cells in the culture medium was measured by SIV p27 antigen enzyme-linked immunosorbent assay (ELISA) (Coulter) [Yamakami et al., 2004; Ami et al., 2005; Someya et al., 2005]. $TCID_{50}$ values were determined by serially diluting plasma and performing quadruplicate infections of M8166 cells. The $TCID_{50}$ assay endpoint was determined on day 10 by SIV p27 antigen ELISA and was calculated by the method of Reed and Muench [1938].

Statistical Analysis

Data are expressed as the mean ± SD. Experimental groups were compared to control groups using the single-factor analysis of variance (ANOVA). If statistical significance ($P < 0.05$) was reached by ANOVA, post hoc comparisons of the means were performed using the Turkey–Kramer test [Kramer, 1956; Someya et al., 2004]. A P-value ≤ 0.05 was considered significant.

RESULTS AND DISCUSSION

In initial experiments conducted to evaluate the efficacy of the electric potential at inactivating HIV-1, HIV-1_{IIIB} was incubated with the indicated concentrations of TiO_2 under UV illumination to induce an electric potential on the TiO_2 surface. The treated virus solution was then filtered to remove TiO_2 particles and incubated with H9 cells for 48 hr. The HIV-1 *env* gene in the infected cells was amplified by DNA polymerase chain reaction (PCR) (Fig. 1B). The optimal concentration of TiO_2 for virus inactivation was found to be 0.25% (w/v), which reduced the generation of the HIV-1 *env*-specific DNA PCR band by 90%. Controls, which received 1 hr of either UV illumination or TiO_2 treatment, showed less than a 10% reduction in the intensity of the HIV-1 proviral band by DNA PCR (data not shown).

The effect of an electric potential induced by UV-illuminated TiO_2 on HIV-1 infectivity was then evaluated using an H9 cell-based assay (Fig. 1C). Virus inactivation, as measured by inhibition of HIV-1 p24 antigen production in infected H9 cells, was similarly optimal at a concentration of 0.25% (w/v) of TiO_2 per reaction mixture. For each concentration tested, the H9 infectivity assay demonstrated levels of virus inactivation similar to those observed in the viral DNA detection experiment, suggesting that the inhibitory effect of UV-illuminated TiO_2 is dependent on direct inactivation of viral particles prior to infection. HIV-1 inactivation was not observed in control experiments in which the virus was pre-treated with TiO_2 but received no UV illumination. While 0.25% (w/v) TiO_2 was found to be optimal in the reaction mixtures, higher concentrations may offer more frequent opportunities for contact between TiO_2 and viral particles. However, surplus TiO_2 could prevent the generation of an electric potential by blocking penetration of the UV light.

Filtration is necessary to trap TiO_2 particles from treated medium using this diffusion-type experiment; thus, the influence of filtration on viral viability was analyzed by counting infected MAGIC-5 cells to evaluate certain UV-irradiated TiO_2 effects (Fig. 1D). The indicated concentration of virus was mixed with 0–1% TiO_2, filtered and used to infect MAGIC-5 cells. The mean infected cell numbers without filtration were 41, 77, 140, and 338 per well with virus concentrations of 25, 50, 100, and 200 ng/ml of p24 antigen, respectively. Consumption by filtration, which includes virus binding on the TiO_2 surface and physical interference by filtration of the virus particles, was approximately 20–25% with 0–0.5% (w/v) TiO_2 at each virus concentration, while that with 1% (w/v) TiO_2 was 55–65%, suggesting that below the concentration of 0.5% (w/v) TiO_2 there is no increase in the physical interference of filtration under these assay conditions.

To further define the conditions required for optimal virus inactivation, we evaluated the intensity and exposure times of UV illumination (Fig. 1E). Two UV light energy levels, 0.8 and 0.4 mW/cm^2, were compared using an H9-based virus infectivity assay and a MAGIC-5 assay as measures of infection. This experiment was performed to evaluate not only differences in the effectiveness of UV intensities, but also the suitability for virus inactivation by observing the results of both short- and long-term cultures. Our results from both studies demonstrated more than 90% inhibition of virus infectivity after 60- and 90-min of exposure, using

0.8 and 0.4 mW/cm^2 of UV light, respectively. The results suggested that higher energy UV contributed stronger virus inactivation effects.

To determine whether conjugation of the HIV-1 receptor CD4 to TiO_2 might enhance virus inactivation following UV illumination, we developed methods to crosslink the CD4 peptide to the surface of TiO_2. Each step in the analysis of the surface properties of TiO_2 was performed using atomic force microscopy (AFM) as described in Figure 2. The surface of untreated TiO_2 was smooth and round (Fig. 2A), as was the surface of TiO_2 at intermediate steps in the conjugation process, that is, immobilization of the first cross-linker with an amino group (Fig. 2B) and of the second with an aldehyde group (Fig. 2C). In contrast, conjugated CD4 peptides were identified as projections from the surface of treated TiO_2 (Fig. 2D).

CD4-conjugated or non-conjugated TiO_2 was then incubated with HIV-1_{IIIB} (100 ng/ml of p24 antigen) for 1 hr before being washed to remove non-adsorbed virions. Scanning electron microscopy (SEM), which has a greater scanning focus than AFM, was used to visualize attached viral particles and evaluate both TiO_2 preparations. HIV-1 virions with a diameter of approximately 100 nm and a calculated surface density of 1×10^8/cm^2 were observed to be attached to CD4-conjugated TiO_2 (Fig. 2E) but were only barely detectable on the surface of CD4-unconjugated TiO_2 (Fig. 2F). Taken together, these observations suggest that the conjugation of CD4 to TiO_2 contributes to the specific binding of HIV-1 to the surface of TiO_2 and that the attached virions will be subsequently inactivated by the electric potentials generated by UV illumination (Fig. 2G). Virus adsorption ability is dependent on the number of CD4 peptides on the TiO_2 surface, which is dependent on the concentration of APTMS in the course of CD4 conjugation. Each CD4-conjugated TiO_2 prepared using the indicated concentrations of APTMS was incubated with medium containing HIV-1_{IIIB} with or without UV illumination for 30 min; then, virus adsorption ability and viral inactivation owing to the combined effects of adsorption and photocatalysis, at each concentration of APTMS, were analyzed. The efficiency of adsorption increased with APTMS concentration (Fig. 2H), whereas the percent inactivation after treatment was approximately 90% at all concentrations of APTM (0.1%, 1%, and 10%) with no significant difference between treatments (Fig. 2I). Figure 2J shows the relative contributions of photocatalysis and adsorption to the total inactivation effect at each concentration of APTMS, suggesting that the total inactivation effect is adsorption dominant, increasing with the concentration of APTMS. The inactivation dependence of the photocatalytic effect is inversely related to the efficiency

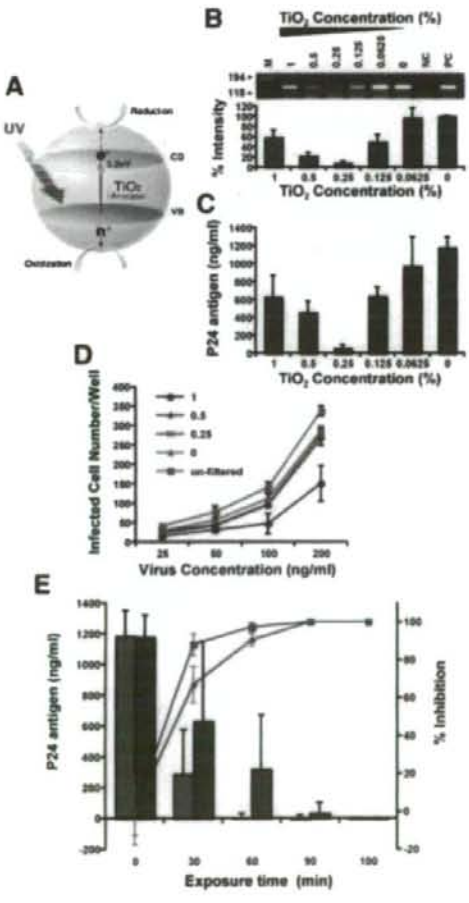

Fig. 1. Inactivation of HIV-1 by the electric potential generated on TiO_2 by UV illumination. **A**: Schematic illustration of photoexcitation of a TiO_2 particle followed by de-excitation events. CB, conduction band; VB, valence band. **B**: Comparison of the efficacy of various TiO_2 concentrations for inhibiting HIV-1 proviral DNA formation in H9 cells. HIV-1_{IIIB} (100 ng/ml of p24 antigen) and the indicated concentrations of TiO_2 particles were exposed to UV light at 0.8 mW/cm^2 for 1 hr. Treated virus preparations were filtered and incubated with H9 cells, and proviral DNA was amplified by PCR 48 hr after infection. The band intensity of the PCR products was analyzed using an image analysis system and compared to an untreated (0 hr) control sample. Each point represents the mean ± SD of duplicate samples from three independent experiments. NC, negative control (uninfected H9 cells); PC, positive control (chronically infected IIIB/H9 cells); M, molecular weight marker (ΦX174/Hae III digest). **C**: Inhibition of HIV-1 infectivity of H9 cells by the electric potential generated on UV-illuminated TiO_2. HIV-1 p24 antigen production was measured in the H9 cell culture medium on day 5 post-infection. Bars represent the mean ± SD of duplicate values from three independent experiments. **D**: Virus consumption by filtration. The indicated titer of HIV-1_{IIIB} and the indicated concentration of TiO_2 powder were mixed in complete medium and filtered. Infectious virus in the filtrated medium was analyzed quantitatively using MAGIC-5 cells. Each point represents the mean ± SD of duplicate values from three separate experiments. **E**: Comparison of two different UV intensities for virus inactivation. TiO_2 at a concentration of 0.25% (w/v) and HIV-1_{IIIB} (100 ng/ml of p24 antigen) in complete medium were exposed to UV light at an intensity of either 0.8 (■) or 0.4 mW/cm^2 (●) for the indicated periods of time and then filtered. The infectivity of virus in the medium was analyzed using an H9 cell culture assay and MAGIC-5 cells. HIV-1 p24 antigen production was measured in the H9 cell culture medium on day 5 post-infection (left scale). Bars represent the mean ± SD of duplicate values from three independent experiments. The results, shown as percent inhibition derived from comparing with untreated control in MAGIC-5 assay, are shown to right scale. (■) 0.8 mW/cm^2; (●) 0.4 mW/cm^2. Each point represents the mean ± SD of values from three separate experiments.

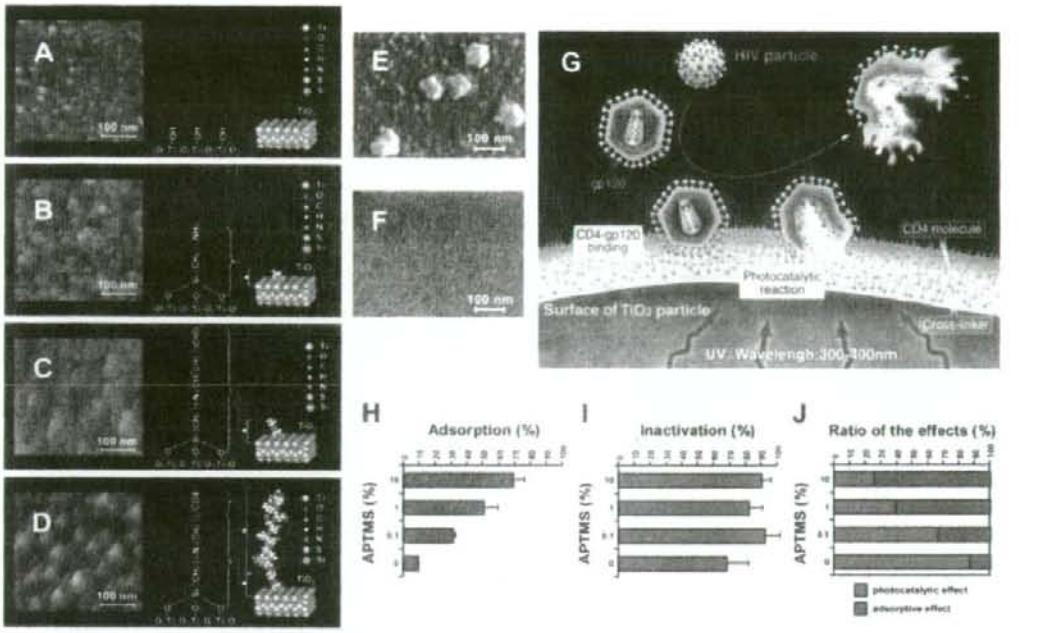

Fig. 2. Atomic force microscopic images of the TiO_2 surface during CD4 chemical conjugation. **A**: Untreated TiO_2. **B**: Immobilization of the first cross-linker with an amino group. **C**: Immobilization of the second cross-linker with an aldehyde group. **D**: CD4-conjugated TiO_2. Three-dimensional structure synthesized by the bio high polymer modeling system (Insight II, Accelrys). The chemical constitution of each step is noted (right side). The distances of the cross-linker and the CD4 peptide ([Cys(Bzl)]^{64}-Fragment 81-92) from the TiO_2 surface are approximately 1.1 nm and 3.9 nm, respectively. A scanning electron micrograph of HIV-1 attached to CD4-TiO_2 and a schematic representation of virus inactivation. CD4-conjugated or non-conjugated TiO_2 that has been incubated with HIV-1_{IIIB} and washed twice with PBS to remove any non-adsorbed virions. **E**: An attached virus with a diameter of approximately 100 nm was observed on the surface of the CD4-TiO_2. **F**: Untreated TiO_2. **G**: Proposed schema for viral inactivation on the surface of CD4-TiO_2 after UV illumination. Determination of an optimal balance of the area between un-conjugated and CD4-congugated on the TiO_2 surface. CD4-conjugated TiO_2 prepared using the indicated concentrations of APTMS in the course of CD4 conjugation were incubated with medium containing HIV-1_{IIIB} with or without UV illumination for 30 min. **H**: Ability of virus adsorption to CD4-TiO_2. **I**: Ability of inactivation as a total effect of both adsorption and photocatalysis of CD4-TiO_2. The results are shown as percent adsorption or inactivation derived from comparisons with untreated controls. Bars represent the means ± SD of values from three independent experiments. **J**: Relative contributions of photocatalysis and adsorption to the total inactivation effects.

of adsorption, owing to a reduction of the un-conjugated area on the TiO_2 surface by conjugation of CD4 peptide. By contrast, an excess of un-conjugated area is capable of reacting nonspecifically with blood constituents in plasma, destroying their intrinsic properties and thereby proving toxic. To maximize both photocatalysis and adsorption, it is important to maintain a balance between the un-conjugated area, which is easily activated by UV, and the CD4-conjugated area, which allows for more efficient virus adsorption. Under the condition of longer periods of incubation, viral particles adsorbed to CD4 molecules would be inactivated and then break away from CD4 peptides. This would be expected to underlie the recovered absorption capability of CD4 peptides to other viral particles. In conclusion, we determined that CD4-conjugated TiO_2 prepared using 0.5% APTMS shows an optimal balance between the two effects and used this concentration of APTMS in subsequent experiments.

CD4 conjugation to TiO_2 was also evaluated for its efficacy at inactivating virus infectivity (Table I). The time required for complete inactivation of virus (either 10 or 100 ng/ml of p24 antigens) was reduced from 45 and 75 min to 30 and 60 min, respectively, indicating that conjugation of CD4 to TiO_2 can speed virus inactivation. Although the anti-viral effects of CD4-TiO_2 did not seem greatly higher than those of un-conjugated TiO_2 in medium, the specificity is very important for clinical applications as it allows for efficient adsorption in plasma.

In other experiments, primary HIV-1 isolates from different clades with tropism for either CCR5 or CXCR4 were evaluated using PBMC-based virus infectivity assays. Among the 25 viruses tested, including 20 primary and 5 typical laboratory isolates, all were completely inactivated by incubation with UV-illuminated CD4-TiO_2 (Table II). Infectivity was lost regardless of co-receptor usage and genetic clade (HIV-1 clades B, B′, E, C, and D). Strikingly, complete inhibition of virus infectivity was achieved using undiluted virus stocks with titers of 500 $TCID_{50}$ (50% tissue culture-infective dose) per milliliter. Similar levels of virus

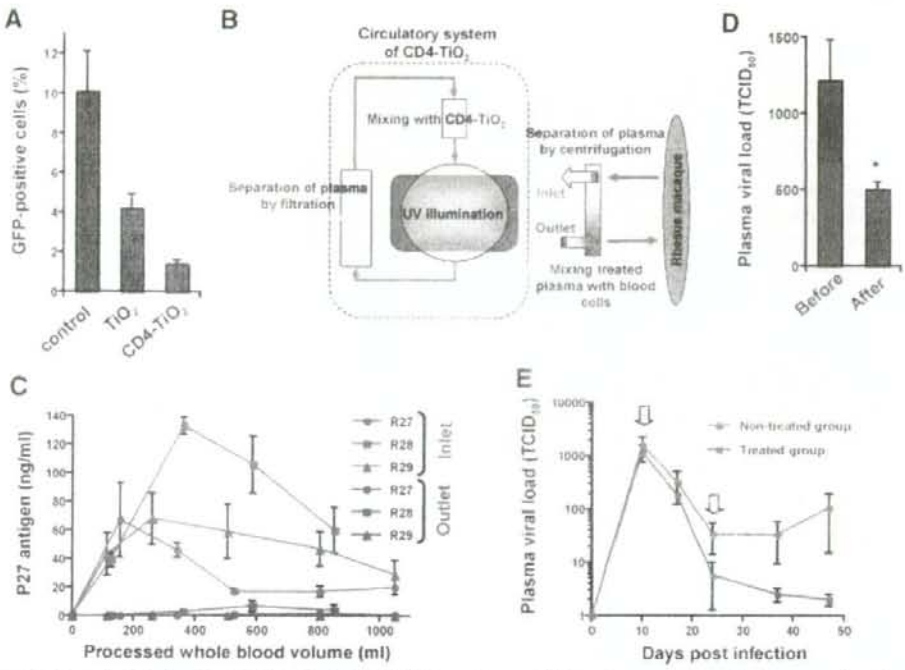

Fig. 3. Inactivation of SIV by the UV-illuminated $CD4\text{-}TiO_2$ with extra-corporeal circulation in SIV-infected rhesus macaques. **A**: Inhibition of SIV infectivity of GHOST-R5 cells by the electric potential generated on UV-illuminated TiO_2 or $CD4\text{-}TiO_2$ in normal human plasma. SIV_{mac239}-containing plasma and the $CD4\text{-}TiO_2$ were exposed to UV light for 30 min. The treated viruses were assessed using a GHOST-R5-based infectivity assay. The number of GFP-positive cells correlates with viral infectivity. Non-treated plasma was used as a control. Bars represent the mean ± SD of duplicate values from three independent experiments and the asterisk represents $P < 0.01$. **B**: An extra-corporeal circulation system for treatment of $CD4\text{-}TiO_2$ with UV illumination. The system consists of a plasma separator applying centrifugation, a $CD4\text{-}TiO_2$ circulatory system with UV illumination, and a plasma separation filter. **C**: Titers of infectious virions in plasma at both an inlet and an outlet of the $CD4\text{-}TiO_2$ circulatory system during the course of the treatment. Plasma was incubated with M8166 cells for 1 hr, and the cells were cultured after removing the plasma. SIV p27 antigen production was measured in the culture medium on day 4 post-infection. **D**: Titers of infectious virions in the bloodstream before and after the treatment. $TCID_{50}$ values were determined by serially diluting plasma and performing quadruplicate infections of M8166 cells. The $TCID_{50}$ assay endpoint was determined on day 10 by SIV p27 antigen ELISA and was calculated using the method of Reed and Muench. Bars represent the mean ± SD of duplicate values from three independent experiments of the three animals and the asterisk represents $P < 0.01$. **E**: Therapeutic treatment with a CD4-conjugated UV-activated photocatalyst controls simian immunodeficiency virus infection in macaques. Animals were treated twice with the UV-activated $CD4\text{-}TiO_2$, first at day 10 and then at day 24 post-infection, as indicated by the bold arrows. Infectious viral titers were determined for the photocatalyst-treated and non-treated groups.

inactivation were also observed using non-passaged plasma viruses from six individuals infected with HIV-1 clade A (NIH1467), clade B (NIH769, NIH770, NIH2713, NIH2976) or clade E (NIH2942). With plasma viral loads of more than 500 $TCID_{50}$, a single treatment with CD4-conjugated and UV-activated TiO_2 deprived all six serum samples of their infectivity. Even with plasma viral loads as high as 5,000 $TCID_{50}$, the treatment inhibited more than 90% of virus infectivity. By contrast, in control experiments non-UV-illuminated TiO_2 had no significant effect on viral inactivation (data not shown). These findings indicate that CD4 conjugation and UV illumination of TiO_2 enables extremely high levels of HIV-1 inactivation of various primary strains, including non-passaged serum viruses. The effects on viruses of serum from chronically infected individuals suggested that the system worked regardless of the presence of serum and antibodies directed against virions that may affect to system in terms of adsorption

TABLE I. Percent Inhibition of Virus Infectivity*

Virus concentration (ng/ml)	TiO_2		$CD4\text{-}TiO_2$	
	10	100	10	100
Exposure time (min)				
0	23 ± 10	0 ± 0	44 ± 35	4 ± 4
15	42 ± 20	8 ± 6	60 ± 32	15 ± 5
30	73 ± 17	70 ± 28	100	86 ± 12
45	100	95 ± 7	100	99 ± 1
60	100	98 ± 3	100	100
75	100	100	100	100
90	100	100	100	100

*Indicated concentration of $HIV\text{-}1_{IIIB}$ and 0.25% (v/w) plain or CD4 conjugated TiO_2 in complete medium was exposed to 0.8 mW/cm^2 UV light. The treated medium was filtered and cultured with H9 cells. p24 antigen level in the culture medium on day 5 after infection was analyzed and the results of % inhibition were derived by comparing to the untreated control. Each value represents the mean ± SD from three separate experiments, each performed in duplicate.

and photocatalysis abilities in clinical settings. As for neutralized viruses, these are no longer the target for this treatment because the viruses do not infect the target cells and also do not attach to TiO_2-CD4. Accordingly, trapping of viral particles via CD4 ensures optimal functioning of TiO_2 as a photocatalyst against HIV targets in serum.

To more thoroughly address the efficacy of the UV-illuminated CD4-TiO_2 in an in vivo model, we used SIV_{mac239} infection in rhesus macaques [Mori et al., 2005; Reimann et al., 2005]. To assess the ability of the CD4-TiO_2 illuminated with UV to inactivate SIV_{mac239}, infectious virus titers in SIV_{mac239}-positive plasma (Control) were compared with those in plasma treated with non-conjugated TiO_2 (TiO_2) or CD4-conjugated TiO_2 (CD4-TiO_2). As shown in Figure 3A, CD4-TiO_2 treatment markedly reduced SIV_{mac239} infectivity, confirming a previous study that reported interactions of the CD4 peptide with both HIV and SIV [Rausch et al., 1992]. No significant reduction was detected in the non-treated SIV_{mac239}-positive plasma of the control group (data not shown). We next devised an innovative CD4-TiO_2 circulatory system with UV illumination, which was equipped with an extra-corporeal circulation system [Ageyama et al., 2003] using a CS3000 blood cell separator (Baxter, Deerfield, IL) to separate plasma and blood cells and to test for the inactivation of virus in the plasma in vivo (Fig. 3B). Employing acutely SIV_{mac239}-infected rhesus macaques (R27, R28 and R29) as experimental animals, we performed initial extra-corporeal circulation 10 days after viral infection. After plasma separation from whole blood was initiated, plasma at the inlet of the circulatory CD4-TiO_2 system for each animal showed infectious virus titers as high as 70–140 ng/ml, (red line with closed symbols in Fig. 3C), with numbers gradually declining with UV-illuminated CD4-TiO_2 treatment. In contrast, plasma at the outlet of the circulatory CD4-TiO_2 system registered zero virus titers throughout the treatment with UV-illuminated CD4-TiO_2 (blue line with closed symbols in Fig. 3C).

As expected, by 10 days after SIV infection, infectious plasma viral load in venous blood from macaques had effectively dropped to 40% of levels observed in the bloodstream after 90–120 min of the initial treatment (Fig. 3D). Following treatment with the extra-corporeal circulation system, renal and liver function results remained unchanged, and no inflammation, cardiomyopathy, thrombotic or hemorrhagic complications were observed in blood.

Twenty-four days after infection, the three animals received a second treatment with the therapeutic photocatalyst. To assess whether the two therapeutic treatments during primary SIV_{mac239} infection of macaques affected the set-point levels of plasma infectious viral copies, we determined infectious virus titers by detecting $TCID_{50}$ values in the plasma of animals. From 4 to 7 weeks after infection, the infectious virus titer in plasma showed greater reductions than those observed in plasma from non-treated control animals (Fig. 3E).

TABLE II. Inactivation of Primary Field Isolates

HIV-1[a]	Tropism[b]	$TCID_{50}$	Percent inhibition[c]
Laboratory isolates			
Clade B			
HIV-MN	X4	500	100
HIV-IIIB	X4	500	100
HIV-SF2	X4	500	100
HIV-AD8	R5	500	100
HIV-89.6	X4, R5	500	100
Primary isolates[d]			
Clade B			
HIV-MNp	X4	500	100
JR-CSF	R5	500	100
JR-FL	R5	500	100
CS2-2	R5	500	100
CS3-5	R5	500	100
CS3-6	R5	500	100
CS4-4	X4, R5	500	100
CS4-8	R5	500	100
CS6-6	R5	500	100
CS6-8	R5	500	100
JCI-1	X4	500	100
JCI-2	X4	500	100
JCI-3	R5	500	100
JCI-5	X4	500	100
Clade B′			
92TH014	R5	500	100
92TH026	R5	500	100
Clade C			
ZMDB33	R5, X4	500	100
Clade D			
NDK	R5	500	100
Clade E			
92TH022	R5	500	100
92TH023	R5	500	100
Plasma viruses			
Clade A			
NIH 1647	R5	5,000	91.6
Clade B			
NIH 769	X4	5,000	90.8
NIH 770	X4	500	100
NIH 2713	X4	100	100
NIH 2976	X4	500	100
Clade E			
NIH 2942	R5	25	100

[a]Clades were determined using the amino acid sequence of the Env-C2-V3 region of viral RNA.
[b]Tropism of the individual viruses to co-receptor CXCR4(X4) and CCR5 (R5) was determined by GHOST cell assay.
[c]Each virus sample was incubated with CD4-TiO_2 under UV illumination for 1 hr and the treated virus solution was further incubated with PHA-activated PBMC. The values represent inhibition of HIV-1 p24 antigen production relative to control samples without the treatment. Results represent the average of three different experiments performed in duplicate.
[d]All the primary viruses shown were passaged within 4 times and titrated only in human PBMC.

Thus, CD4-TiO_2 coupled with UV illumination shows therapeutic promise for HIV-1-infected individuals. We developed the CD4-TiO_2/UV illumination strategy to clinically reduce HIV virions in the bloodstream and serum samples. This is a unique therapeutic immunophysical strategy which can perform physical virus reduction regardless of drug resistance. Reducing the peak value of the infectious plasma viral load in acute

infection might relieve intense viremia which will cause severe damage in target organs and reduction of the set-point levels of infectious virus titer in the bloodstream could help halt the progression to disease states. Additionally, the approach may prove useful when resistant virus load increases despite strict medical regimens and combination with anti viral drugs may exert synergistic effects. Induction of immune response to destructed viral particle promoted by photocatalyst treatment is also expected. Thus physical virus reduction using our CD4-TiO_2/UV illumination strategy could aid recovery from viremia and reconstitution of the exhausted immune system, and we hope that this report will serve as a breakthrough in the treatment of HIV patients faced with increasingly resistant virus.

ACKNOWLEDGMENTS

We are grateful to Kazuyasu Mori for providing SIV_{mac239} and Dr. Masashi Tatsumi for providing MAGIC-5 cells. We thank Yasushi Ami, Takashi Hara, Kenji Someya, Tetsuro Matano, Hirofumi Akari, and Keiji Terao for their helpful discussions. We also thank Yuko Katakai for the handling and care of the monkeys.

REFERENCES

Ageyama N, Kimikawa M, Eguchi K, Ono F, Shibata H, Yoshikawa Y, Terao K. 2003. Modification of the leukapheresis procedure for use in rhesus monkeys (Macaca mulata). J Clin Apher 18: 26–31.

Ami Y, Izumi Y, Matsuo K, Someya K, Kanekiyo M, Horibata S, Yoshino N, Sakai K, Shinohara K, Matsumoto S, Yamada T, Yamazaki S, Yamamoto N, Honda M. 2005. Priming-boosting vaccination with recombinant Mycobacterium bovis bacillus Calmette-Guérin and a nonreplicating vaccinia virus recombinant leads to long-lasting and effective immunity. J Virol 79:12871–12879.

Cecilia D, KewalRamani VN, O'Leary J, Volsky B, Nyambi P, Burda S, Xu S, Littman DR, Zolla-Pazner S. 1998. Neutralization profiles of primary human immunodeficiency virus type 1 isolates in the context of coreceptor usage. J Virol 72:6988–6996.

Chujoh Y, Matsuo K, Yoshizaki H, Nakasatomi T, Someya K, Okamoto Y, Naganawa S, Haga S, Yoshikura H, Yamazaki A, Yamazaki S, Honda M. 2001. Cross-clade neutralizing antibody production against human immunodeficiency virus type 1 clade E and B′ strains by recombinant Mycobacterium bovis BCG-based candidate vaccine. Vaccine 20:797–804.

Conley AJ, Kessler JA II, Boots LJ, Tung JS, Arnold BA, Keller PM, Shaw AR, Emini EA, Williams C, Zolla-Pazner S. 1994. Neutralization of primary human immunodeficiency virus type 1 isolates by the broadly reactive anti-V3 monoclonal antibody, 447-52D. J Virol 68:6994–7000.

Donahue RE, Byrne ER, Thomas TE, Kirby MR, Agricola BA, Sellers SE, Gaudernack G, Karisson S, Lansdorp PM. 1996. Transplantation and gene transfer of the human glucocerebrosidase gene into immunoselected primate CD34+Thy-1+ cells. Blood 87:1644–1653.

Fujishima A, Honda K. 1972. Electrochemical photolysis of water at a semiconductor electrode. Nature 238:37–38.

Gazdar AF, Carney DN, Bunn PA, Russell EK, Jaffe ES, Schechter GP, Guccion JG. 1980. Mitogen requirements for the in vitro propagation of cutaneous T-cell lymphomas. Blood 55:409–417.

Hachiya A, Aizawa-Matsuoka S, Tanaka M, Takahashi Y, Ida S, Gatanaga H, Hirabayashi Y, Kojima A, Tatsumi M, Oka S. 2001. Rapid and simple phenotypic assay for drug susceptibility of human immunodeficiency virus type 1 using CCR5-expressing HeLa/CD4(+) cell clone 1-10 (MAGIC-5). Antimicrob Agents Chemother 45:495–501.

Honda M, Yamamoto S, Cheng M, Yasukawa K, Suzuki H, Saito T, Osugi Y, Tokunaga T, Kishimoto T. 1992. Human soluble IL-6 receptor: Its detection and enhanced release by HIV infection. J Immunol 148:2175–2180.

Honda M, Matsuo K, Nakasone T, Okamoto Y, Yoshizaki H, Kitamura K, Sugiura W, Watanabe K, Fukushima Y, Haga S, Katsura Y, Tasaka H, Komuro K, Yamada T, Asano T, Yamazaki A, Yamazaki S. 1995. Protective immune responses induced by secretion of a chimeric soluble protein from a recombinant Mycobacterium bovis bacillus Calmette-Guerin vector candidate vaccine for human immunodeficiency virus type 1 in small animals. Proc Natl Acad Sci USA 92:10693–10697.

Ishibashi K, Nosaka Y, Hashimoto K, Fujishima A. 1998. Time-dependent behavior of active oxygen species formed on photoirradiated TiO_2 films. J Phys Chem B 102:2117–2120.

Kestler H, Ringler DJ, Mori K, Panicali DL, Sehgal PK, Daniel MD, Desrosiers RC. 1991. Importance of the nef gene for maintenance of high virus loads and for development of AIDS. Cell 65:651–662.

Koyanagi Y, Miles S, Mitsuyasu RT, Merrill JE, Vinters HV, Chen IS. 1987. Dual infection of the central nervous system by AIDS viruses with distinct cellular tropisms. Science 236:819–822.

Kramer CY. 1956. Extension of multiple range test to group means with unequal numbers of replications. Biometrics 12:307–310.

Matano T, Kobayashi M, Igarashi H, Takeda A, Nakamura H, Kano M, Sugimoto C, Mori K, Iida A, Hirata T, Hasegawa M, Yuasa T, Miyazawa M, Takahashi Y, Yasunami M, Kimura A, O'Connor DH, Watkins DI, Nagai Y. 2004. Cytotoxic T lymphocyte-based control of simian immunodeficiency virus replication in a preclinical AIDS vaccine trial. J Exp Med 199:1709–1718.

Mori K, Sugimoto C, Ohgimoto S, Nakayama EE, Shioda T, Kusagawa S, Takebe Y, Kano M, Matano T, Yuasa T, Kitaguchi D, Miyazawa M, Takahashi Y, Yasunami M, Kimura A, Yamamoto N, Suzuki Y, Nagai Y. 2005. Influence of glycosylation on the efficacy of an Env-based vaccine against simian immunodeficiency virus SIVmac239 in a macaque AIDS model. J Virol 79:10386–10396.

Nakasone T, Takamatsu J, Watanabe K, Naganawa S, Someya K, Yoshino N, Kaizu M, Ohsu T, Takizawa M, Izumi Y, Kawahara M, Hara T, Fujimura Y, Yamada K, Nagai Y, Yamazaki S, Honda M. 2000. Decline in the HIV-1 isolation rate in Japan: A 12-year observation. Microbiol Immunol 44:949–952.

Okamoto Y, Eda Y, Ogura A, Shibata S, Amagai T, Katsura Y, Asano T, Kimachi K, Makizumi K, Honda M. 1998. In SCID-hu mice, passive transfer of a humanized antibody prevents infection and atrophic change of medulla in human thymic implant due to intravenous inoculation of primary HIV-1 isolate. J Immunol 160:69–76.

Ou CY, Kwok S, Mitchell SW, Mack DH, Sninsky JJ, Krebs JW, Feorino P, Warfield D, Schochetman G. 1988. DNA amplification for direct detection of HIV-1 in DNA of peripheral blood mononuclear cells. Science 239:295–297.

Pantaleo G, Koup RA. 2004. Correlates of immune protection in HIV-1 infection: What we know, what we don't know, what we should know. Nat Med 10:806–810.

Rausch DM, Lifson JD, Padgett MP, Chandrasekhar B, Lendvay J, Hwang KM, Eiden LE. 1992. CD4(81-92)-based peptide derivatives. Structural requirements for blockade of HIV infection, blockade of HIV-induced syncytium formation, and virostatic activity in vitro. Biochem Pharmacol 43:1785–1796.

Reed LJ, Muench HA. 1938. A simple method of estimating fifty percent endpoints. Am J Hyg 27:493–497.

Reimann KA, Parker RA, Seaman MS, Beaudry K, Beddall M, Peterson L, Williams KC, Veazey RS, Montefiori DC, Mascola JR, Nabel GJ, Letvin NL. 2005. Pathogenicity of simian-human immunodeficiency virus SHIV-89.6P and SIVmac is attenuated in cynomolgus macaques and associated with early T-lymphocyte responses. J Virol 79:8878–8885.

Robinson HI, Amara RR. 2005. T cell vaccines for microbial infections. Nat Med 11:525–532.

Someya K, Xin KQ, Matsuo K, Okuda K, Yamamoto N, Honda M. 2004. A consecutive priming-boosting vaccination of mice with simian immunodeficiency virus (SIV) gag/pol DNA and recombinant vaccinia virus strain DIs elicits effective anti-SIV immunity. J Virol 78:9842–9853.

Someya K, Cecilia D, Ami Y, Nakasone T, Matsuo K, Burda S, Yamamoto H, Yoshino N, Kaizu M, Ando S, Okuda K, Zolla-Pazner S, Yamazaki S, Yamamoto N, Honda M. 2005. Vaccination of rhesus macaques with recombinant Mycobacterium bovis bacillus Calmette-Guerin Env V3 elicits neutralizing antibody-mediated

protection against simian-human immunodeficiency virus with a homologous but not a heterologous V3 motif. J Virol 79:1452–1462.

Weber J, Fenyo EM, Beddows S, Kaleebu P, Bjorndal A. 1996. Neutralization serotypes of human immunodeficiency virus type 1 field isolates are not predicted by genetic subtype. The WHO Network for HIV Isolation and Characterization. J Virol 70:7827–7832.

Yamakami K, Honda M, Takei M, Ami Y, Kitamura N, Nishinarita S, Sawada S, Horie T. 2004. Early bone marrow hematopoietic defect in simian/human immunodeficiency virus C2/1-infected macaques and relevance to advance of disease. J Virol 78:10906–10910.

Ye Y, Si ZH, Moore JP, Sodroski J. 2000. Association of structural changes in the V2 and V3 loops of the gp120 envelope glycoprotein with acquisition of neutralization resistance in a simian-human immunodeficiency virus passaged in vivo. J Virol 74:11955–11962.

Zimmerman K, Schogl D, Plaimauer B, Mannhalter JW. 1996. Quantitative multiple competitive PCR of HIV-1 DNA in a single reaction tube. Biotechniques 21:480–484.

FEBS Letters 582 (2008) 4053–4058

Identification of the P-TEFb complex-interacting domain of Brd4 as an inhibitor of HIV-1 replication by functional cDNA library screening in MT-4 cells

Emiko Urano[a,b], Yumi Kariya[a], Yuko Futahashi[a], Reiko Ichikawa[a], Makiko Hamatake[a], Hidesuke Fukazawa[c], Yuko Morikawa[b], Takeshi Yoshida[d], Yoshio Koyanagi[d], Naoki Yamamoto[a], Jun Komano[a,*]

[a] *National Institute of Infectious Diseases, 1-23-1 Toyama, Shinjuku-ku, Tokyo 162-8640, Japan*
[b] *Graduate School of Infection Control Sciences, Kitasato University, Shirokane 5-9-1, Minato-ku, Tokyo 108-8641, Japan*
[c] *Department of Bioactive Molecules, National Institute of Infectious Diseases, 1-23-1, Toyama, Shinjuku-ku, Tokyo 162-8640, Japan*
[d] *Laboratory of Viral Pathogenesis, Institute for Virus Research, Kyoto University, Kyoto 606-8507, Japan*

Received 26 August 2008; revised 10 October 2008; accepted 21 October 2008

Available online 7 November 2008

Edited by Ivan Sadowski

Abstract We conducted a phenotypic cDNA screening using a T cell line-based assay to identify human genes that render cells resistant to human immunodeficiency virus type 1 (HIV-1). We isolated potential HIV-1 resistance genes, including the carboxy terminal domain (CTD) of bromodomain-containing protein 4 (Brd4). Expression of GFP-Brd4-CTD was tolerated in MT-4 and Jurkat cells in which HIV-1 replication was markedly inhibited. We provide direct experimental data demonstrating that Brd4-CTD serves as a specific inhibitor of HIV-1 replication in T cells. Our method is a powerful tool for the identification of host factors that regulate HIV-1 replication in T cells.

Keywords: HIV-1 replication; Host factor; cDNA library; Brd4; P-TEFb complex; Tat-dependent LTR transcription

1. Introduction

The identification of specific molecular interactions required for efficient HIV-1 replication should provide clues towards improved understanding of the mechanisms of viral pathogenesis, as well as of host defence against HIV-1. In addition, this may help design highly specific inhibitors against HIV-1. Genome-wide screening for HIV-1 replication regulatory factors has been attempted by using various experimental approaches. Most of them were based on adherent epithelial cells, because these cells exhibit higher transduction efficiencies (by transfection or by viral vector transfer) when compared with T cell lines [1,2]; however, cells of epithelial origin are not relevant hosts for HIV-1 in vivo. Furthermore, viral vectors pseudotyped with vesicular stomatitis virus-G (VSV-G) are often used for screening purposes, instead of wild-type HIV-1. These vectors enter cells via the VSV-G-restricted route, which is different from the HIV-1 envelope-mediated entry pathway. These factors constitute potential caveats of these assays.

To overcome these potential problems, we carried out a phenotypic screen to identify human cDNAs that confer resistance to HIV-1 replication, without affecting cell proliferation. The assay was performed in a human T cell line, a physiologically relevant host, stably transduced with a human cDNA library. We isolated several potential HIV-1 resistance genes successfully, many of which were not known as HIV-1 regulatory factors. In this work, we studied Brd4 in detail to demonstrate the applicability of our phenotype screening. Our study of Brd4-CTD suggests the presence of a potential anti-HIV-1 drug target in the host transcription regulator cyclin T1 (CCNT1).

2. Materials and methods

2.1. Cells and transfection

Cells were maintained in RPMI 1640 medium (Sigma, St. Louis, MA) supplemented with 10% fetal bovine serum (Japan Bioserum, Tokyo), 50 U/ml penicillin, and 50 μg/ml streptomycin (Invitrogen, Tokyo, Japan), and then incubated at 37 °C in a humidified 5% CO_2 atmosphere. Cells were transfected with Lipofectamine 2000 according to the manufacturer's protocol (Invitrogen).

2.2. Plasmid construction

The Brd4-CTD was amplified from 293T RNA by reverse transcriptase PCR (RT-PCR) using the primers 5′-AGATCTCTCATCCGACCACCCCCTCCTCC-3′ and 5′-TCAGGATCCCGAAAAGATTTTCTTCAAATATTG-3′. The BglII–BamHI fragment of the PCR product was cloned into the corresponding restriction sites of the pEGFP-C2 (Clontech, Palo Alto, CA). The XhoI–MfeI fragment from the resulting plasmid was cloned into the corresponding restriction sites of the pCMMP KRAB vector, creating the pGFP-Brd4-CTD. The cDNA encoding firefly luciferase (Luc^+) was amplified by PCR from the pGL3-Basic (Promega, Madison, WI) using the primers 5′-ACCGGTCTCGAGGGCCACCATGGAAGACGCCAAAAACATAAAGAAAGG-3′ and 5′-GAATTCGGATCCTTACACGGCGATCTTTCCGCCCTTCTTGGCC-3′. The PCR product was digested with AgeI and BamHI, and cloned into the corresponding sites of the pCMMP GFP vector, generating the pCMMP Luciferase. The BamHI–XhoI fragment of pLenti6/V5-GW/lacZ (Invitrogen) was removed, and Luc^+ was inserted with BglII and SalI sites artificially attached at its extremities, creating the pLenti Luciferase. Other plasmids used in this study were described previously [3,4].

*Corresponding author. Fax: +81 3 5285 5037.
E-mail address: ajkomano@nih.go.jp (J. Komano).

0014-5793/$34.00
doi:10.1016/j.febslet.2008.10.047

2.3. Selecting human cDNAs that confer resistance to HIV-1

The lentiviral vector carrying an hPBL cDNA library was described previously [5]. MT-4 cells (1×10^6) transduced with the cDNA library were infected with HIV-1_{HXB2} propagated in MT-2 cells, by resuspending MT-4 cells in a viral preparation containing 70–1250 ng/ml p24 viral capsid antigen in 20 ml of culture medium for 30 min at room temperature with continuous mixing. Anti-CD4 magnetic beads (0.5–1.0×10^7; Dynal, Oslo, Norway) were added to the cell suspension to prevent cell-to-cell contact, and the cells (1×10^5 cells per well in 200 μl of culture medium) were plated in flat-bottomed 96-well plates. At 3–4 weeks post-infection, cells from four wells positive for cell outgrowth were pooled and genomic DNA was extracted. The cDNA inserts were PCR-amplified and sequenced using primers described previously [5].

2.4. Generation of viruses and infection

Viruses were produced as described previously [3,4]. Human T cell lines (MT-4 and Jurkat cells; 1×10^5 cells) were incubated with 500–1000 μl of MLV preparations in the presence of 8 μg/ml polybrene for 1 h at 4 °C with continuous agitation. For HIV-1 infection, 1×10^5 cells were incubated with an HIV-1-containing culture supernatant (*ca.* 5–5000 pg p24), for 30 min at room temperature. HIV-1 replication was monitored as described previously [3,4].

2.5. Western blotting

Western blotting was performed according to techniques described previously [4]. The following antibodies were used: anti-CCNT1 (ab2098, Abcam, MA), anti-Brd4 (ab46199, Abcam), anti-GFP (MAB3580, Chemicon International, Temecula, CA or 632381, Clontech), anti-p24 (183-H12-5C, NIH AIDS Research and Reference Reagent Program), anti-HEXIM1 (ab25388, Abcam), anti-Bip/GRP78 (clone 40, BD Transduction Laboratories), and EnVision+ system (Dako, Glostrup, Denmark).

2.6. Reporter assay

The 293T cells grown in 48-well plates were co-transfected with 20 ng of pLTR-Luc or pCMMP Luciferase, together with pGFP-Brd4-CTD. The total amount of transfected DNA was adjusted by pCMMP GFP. To measure the effect of Tat, cells were co-transfected with 100 ng of pSVtat in addition to the above-mentioned plasmids. Cells were replated in 96-well plates in triplicate at 2–4 h post-transfection. Luciferase activity was measured 48 h after transfection using the Dual-Glo assay kit (Promega).

2.7. RT-PCR

RT-PCR was performed as described previously [4]. For amplification of HIV-1 mRNA, forward (5′-CTCGACGCAGGACTCGGCTTGC-3′) and reverse (5′-AGTTCCACTCCTGCCCAAGTATCC-3′) primers were used. The mRNA encoding glyceraldehyde-3-phosphate dehydrogenase (GAPDH) was amplified using the primers 5′-GTGGAAGGACTCATGACCACAGTC-3′ and 5′- CATGTGGGCCATGAGGTCCACCAC-3′.

2.8. Quantitative real-time PCR

The real-time PCR reaction was performed as described previously [4]. Amplifications were performed using the QuantiTect SYBR Green RT-PCR/PCR Kit (QIAGEN). To estimate the amount of integrated HIV-1 DNA, Alu-LTR PCR was performed as described previously [6] using the following primers: first PCR reaction, 5′-AACTAGGGAACCCACTGCTTAAG-3′ and 5′-TGCTGGGATTACAGGCGTGAG-3′; and second PCR reaction, 5′-AACTAGGGAACCCACTGCTTAAG-3′ and 5′-CTGCTAGAGATTTTCCACACTGAC-3′.

3. Results

To isolate cDNA clones that confer resistance to HIV-1 without negatively affecting cell proliferation, we performed phenotype screening using MT-4 cells stably transduced with a lentiviral vector carrying a cDNA library from human peripheral blood lymphocytes (hPBL). The complexity of the lentiviral cDNA library was on the order of 10^6. The lentiviral vector encoded a GFP expression cassette. Approximately 70% of the MT-4 cells became GFP-positive after infection of the lentiviral vector, suggesting that a portion of the cells were infected with multiple lentiviral vectors. The GFP-positive cells were collected using a FACS sorter and subsequently exposed to replication-competent HIV-1. The surviving cell clones were propagated and their transduced cDNAs were examined. The average length of hPBL cDNA in the lentiviral vector was ~0.7 kbp, which is shorter than the average human cellular mRNA length (~2 kbp). A gene was considered an innate

Table 1
Summary of cDNAs recovered in an HIV-1-resistant phenotype screening in MT-4 cells.

Gene category	# of independent clones	Frequency (%)	Frequently isolated genes[a] (# of independent clones)
Metabolism	16	24.6	Haemoglobin (7) Pyridoxal kinase, PDXK (3)
Transcription	7	10.8	Bromodomain containing 4, Brd4 (3) Zinc finger protein 26, ZNF26 (3)
Ribosomal proteins	7	10.8	Ribosomal protein L14, RPL14 (3)
Signal transduction	7	10.8	Zinc finger protein 36, ZFP36L2 (2) transducin beta-like 1X-linked, TBL1X (1)[c]
Trafficking	6	9.2	Chromosome 22 open reading frame 5, C22orf5 (1)[c] Chromosome 9 open reading frame 86, C9orf86 (1)[b] Chromosome 1 open reading frame 142, C1orf142 (1)[b] Nedd4-binding partner 3, N4BP3 (1)
Immunology	2	3.1	MHC class II, DR alpha (1)
Oncogenesis	2	3.1	AXIN1 up-regulated, AXUD1 (1)[c]
Glycosylation	2	3.1	Hyaluronan and proteoglycan link protein 3, HAPLN3 (1)
Differentiation	2	3.1	Jumonji AT rich interactive domain 2, JARID2 (1)
Cytoskeleton	2	3.1	Beta actin (1)
Cell cycle control	1	1.5	CWF19-like 1, CWF19L1 (1)
Apoptosis	1	1.5	Chromosome 2 open reading frame 28, C2orf28 (1)
DNA repair	1	1.5	Non-SMC element 1 homolog, NSMCE1 (1)[b]
Non-ORF coding	9	13.8	–
Total	65	100.0	–

[a]All the clones isolated more than three times are listed. A representative clone is shown for categories with a few candidates.
[b]These genes exhibited regulatory functions on HIV-1 production.
[c]These genes exhibited no effect on HIV-1 production.

negative factor for HIV-1 replication if the full-length open reading frame (ORF) was recovered. Alternatively, if a portion of a gene was recovered, the full-length gene was considered a potential positive factor for HIV-1 replication. We recovered 65 independent cDNA clones (43 genes, Table 1). A number of cDNAs encoded abundant cellular transcripts, including haemoglobin. In addition, cDNAs encompassing non-ORFs were isolated. The isolation of these cDNAs was likely due to the infection of a single cell with multiple cDNA-transducing lentiviral vectors, one of which encoded an HIV-1 resistance gene. If we disregard these cases, 26 genes were potential HIV-1 regulatory gene candidates, of which seven were examined for a potential HIV-1 regulatory functions as shown in Fig. 2. Four genes exhibited HIV-1 regulatory phenotypes (4/7 genes, 57.1%; Table 1). In addition to Brd4-CTD, C9orf86 and NSMCE1 scored as positive factors for HIV-1 replication, and C1orf142 was scored as a negative factor. This suggested that our screening was successful in selecting for HIV-1 regulatory genes. While each candidate gene will be studied in detail in future studies, here we focused on Brd4.

Brd4 was chosen for three reasons: (1) three independent Brd4 cDNAs were recovered; (2) Brd4 binds to the CCNT1/T2-bearing P-TEFb complex [7,8]; and (3) 13 independent Brd4 cDNA clones (13/42 clones, 31.0%) were isolated from a similar experiment in which the cDNA library from an *Oryctolagus cuniculus* kidney derived cell line was used. All the three Brd4 cDNA clones encoded Brd4-CTD: two encoded amino acids (aa) 1260–1362 and the third encoded aa 1209–1362 (Fig. 1A). The first two clones were translated using the Met-encoding codon at Brd4 nucleotide position 3778–3780, and the third was translated from the aberrant start codon in the primer upstream of the Brd4 ORF 3628 nt. To our surprise, aa fragment 1209–1264 of Brd4 was recently reported as an interactor of CCNT1 that inhibits Tat-dependent LTR-driven transcription [9]; however, the specific effect of this region on HIV-1 replication in human T cells was not fully investigated.

We hypothesized that the repression of HIV-1 replication in MT-4 cells may be due to the selective inhibition of viral gene transcription by Brd4-CTD. To test this, we cloned Brd4-CTD spanning aa 1209-1364 into a retroviral plasmid and fused GFP to its carboxy-terminus (GFP-Brd4-CTD, Fig. 1B). Confocal microscopy revealed that GFP-Brd4-CTD was localized mainly in the cytoplasm of MT-4 cells, with some signal found in the nucleus (Fig. 1C). A transient transfection assay revealed that the expression of GFP-Brd4-CTD modestly enhanced the luciferase expression driven by both the LTR and CMV promoters (Fig. 1D). In the presence of Tat, LTR

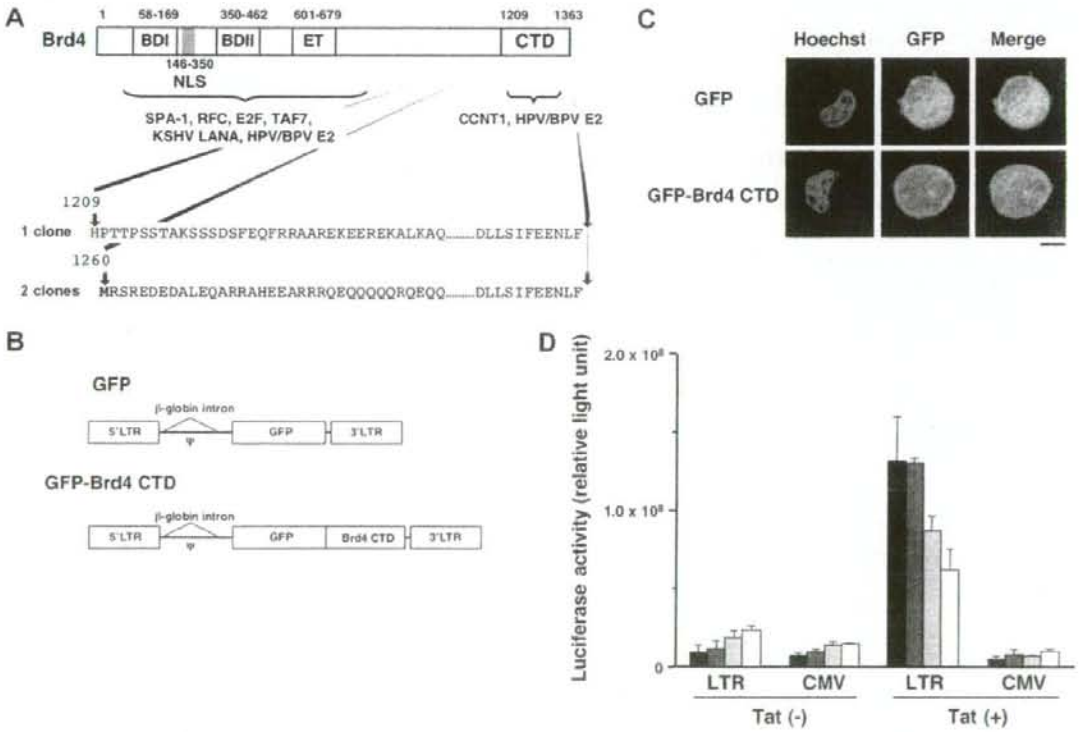

Fig. 1. Specific inhibition of Tat-dependent LTR transcription by GFP-Brd4-CTD. (A) Functional properties of the Brd4 domains and isolated Brd4 cDNAs. (B) Construction of MLV vector-based mammalian expression plasmids encoding GFP or GFP-Brd4-CTD. (C) Confocal microscopy images of MT-4 cells stably expressing GFP or GFP-Brd4-CTD. Green and blue represent GFP and the Hoechst 33258-stained nuclei, respectively. Magnification, 630×; scale bar, 5 μm. (D) Effect of GFP-Brd4-CTD on LTR and CMV promoter activities in the absence or presence of the Tat expression plasmid. Cells transfected with 0, 16, 80, and 400 ng of pGFP-Brd4-CTD correspond to black, dark gray, light gray, and white bars, respectively. Representative data from five independent experiments are shown.

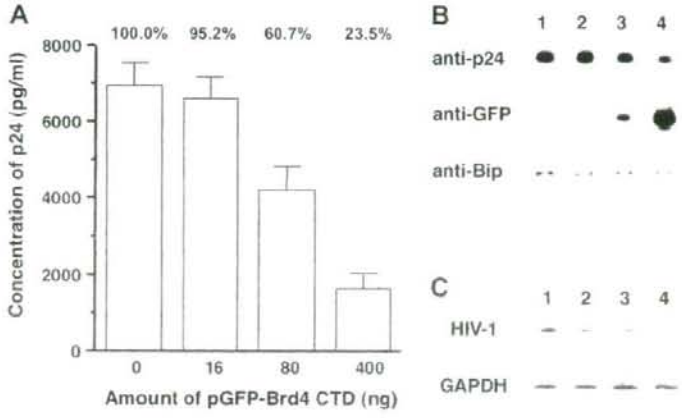

Fig. 2. Inhibition of HIV-1 production by GFP-Brd4-CTD. (A) Viral production was quantified by ELISA detecting p24 viral antigen. The relative decrease in viral levels are indicated on the top of the graph. (B) The viral protein levels in transfected cells were analyzed by Western blotting using the antibodies indicated. (C) The viral spliced transcript and GAPDH mRNA were amplified by RT-PCR. Lanes 1–4 in B and C correspond to the amount of pGFP-Brd4-CTD (0, 16, 80, and 400 ng, respectively). Quantification of these data is summarized in Table 2.

activity was markedly enhanced. When the GFP-Brd4-CTD expression vector was co-transfected, the Tat-dependent enhancement of LTR promoter-driven luciferase expression decreased. A similar trend was not observed for the CMV promoter. These data suggest that the Brd4-CTD specifically limits Tat-dependent LTR transcription.

We also investigated the effect of GFP-Brd4-CTD expression on HIV-1 production by using a proviral DNA mimicking the late phase of the viral life cycle. Consistent with the results described above, transfection of HIV-1 proviral DNA together with an increasing amount of the GFP-Brd4-CTD expression vector led to a decrease of viral yield, as well as of the levels of viral protein and mRNA in the transfected cells (Fig. 2). The viral RNA levels dropped in parallel with the protein levels, as demonstrated by real-time RT-PCR analysis (Fig. 2C and Table 2). These data suggest that GFP-Brd4-CTD inhibits HIV-1 production by blocking viral transcription.

To confirm the blockage of HIV-1 replication by Brd4-CTD, GFP-Brd4-CTD was transduced into MT-4 and Jurkat cells using an MLV-based vector (Fig. 3A). Green fluorescence indicated that the efficiency of MLV-mediated gene transduction in MT-4 cells was >90%, with a lower transduction efficiency observed in Jurkat cells, as estimated by FACS analysis. The GFP-positive Jurkat cells were collected using a FACS sorter. The expression of GFP and GFP-Brd4-CTD was verified by Western blot analysis (Fig. 3B). The expression levels of transcription-related gene products were not detectably affected by the constitutive expression of GFP-Brd4-CTD (Fig. 3B). In addition, there was no detectable difference in the levels of cell-surface HIV-1 receptors (CD4 and CXCR4), cell morphology, and cell proliferation rates between GFP- and GFP-Brd4-CTD-expressing cells (Fig. 1C and Supplementary data). We found that HIV-1 replicated less efficiently in GFP-Brd4-CTD-expressing cells than in GFP-expressing cells, in both cell lines tested, which confirms the HIV-1-resistant phenotype of MT-4 cells (Fig. 3C). The efficiency of viral genome integration into GFP-Brd4-CTD-expressing cells was indistinguishable from that of GFP-expressing cells (103.2 ± 24.1%) as examined by Alu-LTR PCR, suggesting that the early phase of the viral life cycle was not blocked by GFP-Brd4-CTD.

4. Discussion

Our phenotype screening method proved to be a powerful tool because a human T cell line was subjected to HIV-1 resistance screening by stable and non-transient introduction of a human cDNA library, and because wild-type HIV-1 was used; thus, the effect of candidate gene expression on cell proliferation was less of a concern in this system when compared with transient assay systems. In addition, HIV-1 inhibitory genes were isolated at a frequency of ~15% (4/26 genes), 75% of which were novel. We therefore believe that our system is remarkable in selecting genes that confer HIV-1 resistance in T cells. By applying this assay to other cDNA libraries, we

Table 2
Effect of GFP-Brd4-CTD on viral production examined by quantitative real time RT-PCR and ELISA.

pGFP-Brd4-CTD (ng)	HIV-1 mRNA (copy)[a]	GAPDH mRNA (copy)[a]	Ratio (HIV-1/GAPDH)	Normalized (%)[b]	p24 ELISA (%)[c]
0	274250	261750	1.048	100.0	100.0
16	221600	228850	0.968	92.4	95.2
80	138050	311450	0.443	42.3	60.7
400	120850	347750	0.348	33.2	23.5

[a]Copy per 100 ng total cellular RNA.
[b]Relative reduction of HIV-1 mRNA considering pGFP-Brd4-CTD 0 ng as 100%.
[c]See Fig. 2.

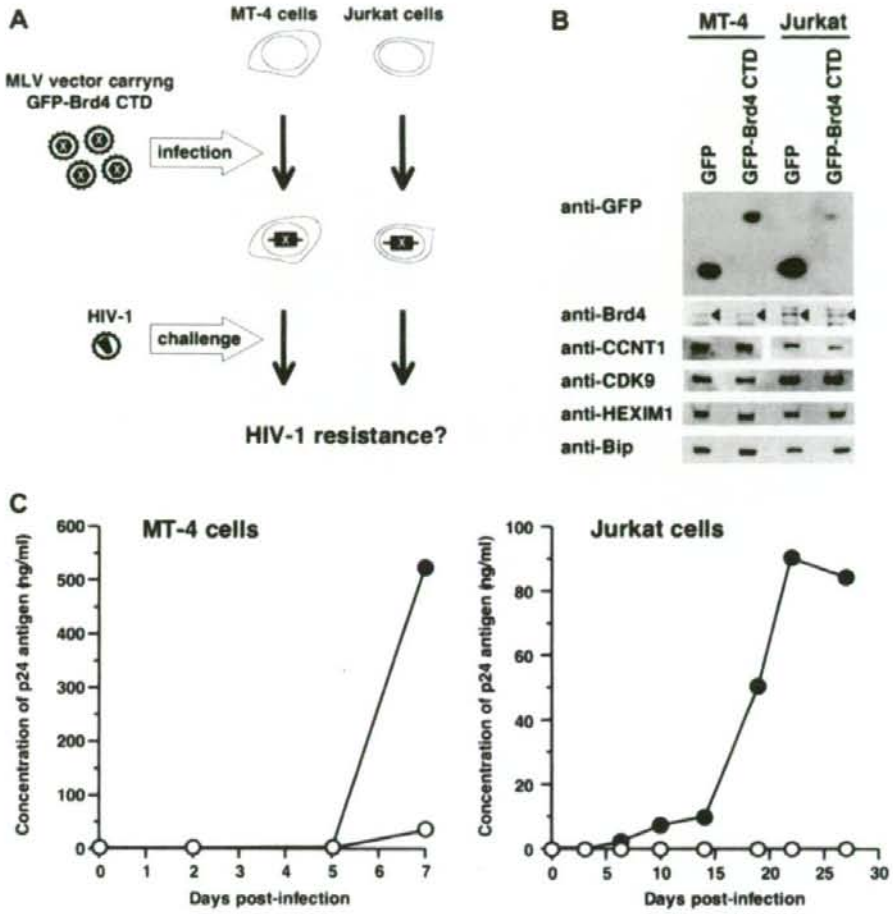

Fig. 3. Constitutive expression of GFP-Brd4-CTD limited the replication of HIV-1. (A) Experimental design. MT-4 and Jurkat cells were transduced with an MLV vector expressing GFP-Brd4-CTD. Cells were challenged by HIV-1 and the efficiency of viral replication was examined. (B) Western blot analysis of the expression levels of GFP, GFP-Brd4-CTD, Brd4 (arrowhead), CCNT1, CDK9, HEXIM1, and BiP in established MT-4 and Jurkat cells. (C) HIV-1 replication kinetics in MT-4 and Jurkat cells constitutively expressing GFP (black circles) or GFP-Brd4-CTD (white circles). Representative data from two independent experiments are shown.

may be able to isolate novel cellular factors that regulate HIV-1 replication.

The assessment of the selective impact of altered candidate gene expression or function on HIV-1 replication (without the alteration of cell proliferation) is critical to the identification of cellular molecular targets for novel anti-retroviral drugs. We demonstrated that Brd4-CTD was a specific silencer of HIV-1 replication, and verified that it effectively blocked HIV-1 replication in multiple human T cell lines without affecting cell proliferation. Our data indicate that primate lentiviral replication is more heavily dependent on the CCNT1-containing P-TEFb complex than cellular gene transcription, which is consistent with previous findings [4,10–11]. This implies that HIV-1 replication can be controlled by selectively restricting the CCNT1-containing P-TEFb complex. Our transcription assay indicated that the Brd4-CTD is not an inhibitor of the P-TEFb complex, but is rather a functional Tat inhibitor. Previous biochemical studies have suggested that Brd4-CTD and Tat bind to CCNT1 in a reciprocally exclusive fashion [7,9]. Given that the binding regions of these two proteins do not overlap, Brd4-CTD may be an allosteric inhibitor of the Tat-CCNT1 interaction. Taken together, our results indicate that the Brd4-interacting region of CCNT1 is a potential molecular target for the development of a novel HIV-1 inhibitor.

Acknowledgements: This work was supported by the Japan Health Science Foundation, the Japanese Ministry of Health, Labor and Welfare (H18-AIDS-W-003) and the Japanese Ministry of Education, Culture, Sports, Science and Technology (18689014 and 18659136).

Appendix A. Supplementary data

Supplementary data associated with this article can be found, in the online version, at doi:10.1016/j.febslet.2008.10.047.